

CU 508845
7/82

IN-92
64792-CR
P.32

FINAL REPORT

SOLAR DYNAMICS AND G-MODES

NASA Contract NAS5-28196

**Jane B. Blizard, Principal Investigator
Astrophysical, Planetary, and
Atmospheric Sciences, Box 391
University of Colorado
Boulder, CO 80309**

**Charles L. Wolff, Technical Director
NASA Goddard Space Flight Center, Code 610.1
Greenbelt, MD 20771**

August, 1984-February, 1987

February 10, 1987

**(NASA-CR-180737) SOLAR DYNAMICS AND G-MODES
Final Report (Colorado Univ.) 32 pCSCL 03B**

N88-14911

**Unclas
G3/92 0064792**

Table of Contents

	<u>Page</u>
Table of Contents	iii
Acknowledgements	ii
Disclaimer	ii
Publications Issued Under Contract	ii
List of Figures	i
List of Tables	i
1 R-Mode Oscillations in the Convective Zone of the Sun	1
1.1 Introduction	1
1.2 Eddy Viscosity	1
2 Sunspot Record and Fast Fourier Transforms	6
2.1 Zurich Sunspot Number Record	6
2.2 Greenwich Sunspot Area Record	6
3 Evaluation of FFT's with Wolff & Hickey (1986) Model	16
4 External Force	20
4.1 Magnitude in terms of Luminosity	20
4.2 Time Span of Torque in External Sector	22
4.3 Half-power Calculation	25
4.4 North-South Asymmetry	26
5 Bibliography	28

Acknowledgements

The author expresses gratitude to Charles L. Wolff of NASA Goddard Space Flight Center, Greenbelt, Maryland, under whose sponsorship this work was performed as partial fulfillment of Contract NAS5-28196. Further acknowledgement is due to the APAS Dept. of the University of Colorado for assistance in preparation of the line drawings and typing of the text, and to JILA, U. of Colorado for copying and reproduction.

The author acknowledges many useful discussions with (and much reference material supplied by) Charles L. Wolff and John P. Cox. Many thanks to L. Jane Twigg for conversion of Zurich sunspot data from magnetic tape to floppy disks.

Many thanks for helpful discussions are due to C.J.Hansen, Dean Pesnell, E.R.Benton, C.Sawyer, J.W.Warwick, K.D.Wood, Chela Kunasz, and Olivia Briggs of CU, and to H.H.Sargent III, P. McIntosh, & M. Dryer of NOAA.

Finally, many thanks to Mark Lund for extensive computer operation and programming during the course of the investigation, and for reading the entire manuscript.

Disclaimer

The contents of the report reflect the viewpoint of the author who is responsible for the accuracy of the results presented. Publication of this technical report does not necessarily reflect the views or policy of NASA Goddard Space Flight Center or the U.S.Government.

Publications issued under NASA Contract NAS5-28196:

1. Blizard, J. B., "Viscosity Losses in the Solar Convection Zone," B.A.A.S. 17#2 p. 610 (1985)
2. Wolff, C. L. & Blizard, J. B., "Properties of r-Modes in the Sun," Sol. Phys. 105 1-15 (1986)
3. Blizard, J. B., & Wolff, C. L., "Short Periods in the Power Spectrum of Sunspot Number--16 days to one year, and r-mode oscillations in the sun," P.A.S.P. 98 1100 (1986)
4. Blizard, J. B., & Wolff, C. L., "R-mode Oscillations in the Sun," Lecture Notes in Physics # :Stellar Pulsation," Springer-Verlag, NY 1987.

List of Figures

Page

1.1 Schematic fluid motion of r-modes	3
2.0 Twentieth century sunspot cycles	7
2.1 Fast Fourier transforms, sunspot area: cycles 14, 15	8
2.2 " " " " " cycles 16, 17	9
2.3 " " " " " cycles 18, 19	10
2.4 " " " " " cycles 20, 21	11
2.5 Fast Fourier transforms, sunspot number: cycles 14, 15	12
2.6 " " " " " cycles 16, 17	13
2.7 " " " " " cycles 18, 19	14
2.8 " " " " " cycles 20, 21	15
3.1 Mean Fourier spectrum, cycles 14-21, spot area, and model lines from Wolff & Hickey (1987)	18
4.1 Duration of F_h over 5 day period	20
4.2 Torque exerted on sun's equatorial bulge by a planet	20
4.2.1 Plan view of solar system, 1976	23
4.3.1 Two point masses; half-value of g_{max}	25
4.4.1 Relative spotted areas of N-S hemispheres; latitude of outer planets, 1830-1960	27
4.4.2 Asymmetry of N-S hemispheres 1943-1977; latitude of outer planets relative to solar equator	27

List of Tables

1.1 Spherical harmonic terms of stress tensor	3
1.2 Eigenfunctions (l,m,n) numerically calculated for 140 zones in solar convection zone	4
1.3 Sidereal rotation of r-modes; repetition of identical flow fields viewed from Earth	5
3.1 Expected frequencies & observed amplitudes for 8 solar cycles: spectra of spot area	17
4.1 Days two planets are within 1/2 radian (Allen, 1973)	24
4.2 Days two planets are within 1/2 radian (Astron. Almanac)	24
4.3 Periods of the planets viewed from the subsolar point	24
4.4 Relative amplitudes of torque of planets on sun	24
4.4.1 Longitude of the outer planets, 1790-2000	27

1 R-MODE OSCILLATIONS IN THE CONVECTIVE ZONE OF THE SUN

1.1 INTRODUCTION. P-modes and g-modes have been actively studied since it first appeared that the Sun might be oscillating in modes of global scale. But there is another type of global mode, called r-modes from their similarity to the Rossby waves in meteorology. These toroidal modes have very long periods comparable to the sun's rotation period, while the p- and g-modes have periods of minutes or hours, and their motion is controlled by the Coriolis force, whereas for the p- and g-modes the restoring forces are compression and buoyancy.

Also the motion of r-modes is almost purely toroidal (non-radial), while the p- and g-mode motions are mainly spheroidal (radial). Disturbance in the Sun would excite both toroidal and spheroidal components. We cannot continue to ignore the r-modes in solar physics. The r-modes are thought to be damped in the Sun. But damping does not remove them from observational interest. The solar envelope is in constant motion. Differential rotation drives eddies whose vertical component would be a source for r-modes. Lower angular harmonics (Fig. 1.1) would also be expected to be generated by the eddy motion of horizontal flows at the top of large convection cells and especially the cells of global scale. Any detection of r-modes would give an important new probe of the sun's interior rotation.

1.2 EDDY VISCOSITY. We computed various properties of r-modes that would occupy the solar convection zone. Large scale motions in the solar envelope are non-adiabatic since they are immersed in a turbulent medium.

If simple diffusion theory applies, an energy loss can be computed from the coefficient of eddy viscosity $\eta = 1/3 \rho V_{\text{con}} L$, where $V_{\text{con}} = L/t_c$ (mixing length/conv. overturning time). We calculated values of this using the solar convective zone model of Baker & Temesvary (1966). Following Landau & Lifshitz, viscous damping acting alone will change the energy of an r-mode in one oscillation period by

$$E_v = -\frac{\pi}{\sigma} \int_{\text{vol}} dV \eta \sum_{i,j} (D_{ij})^2 \quad (1.1)$$

where the deformation tensor for large scale velocity is

$$D_{ij} = 1/2 \left(\frac{\partial v_j}{\partial r_j} + \frac{\partial v_j}{\partial r_i} \right) \quad (1.2)$$

In spherical coordinates for $l=1$ and both $l=2$ cases, the summation of D_{ij} terms give compact expressions which can be integrated over angle. Assuming that η depends only on radial distance, $x=r/R_0$,

$$E_v = -2\pi \delta R_0 \int dx x^2 \eta \delta_l \quad (1.3)$$

where δ is the term for the angular harmonic (Table 1.1). This approach requires the r-mode to have an oscillation period, $P \gg t_c$ (conv. overturning time), a long wavelength $X \gg L$ (mixing length), and a viscous energy dissipation $E_v \ll E$ (total energy).

Special attention must be given to layers close to the base of the convective zone because of a possible anisotropic viscosity coefficient there. In the lower part of the convection zone, most of the energy would be lost to viscosity in a single oscillation period. Fortunately, this lower region is not very important to the mode as a whole; only about 10% of the undamped linear mode energy would lie below this region (at about $0.85 R_\odot$, where the base of the CZ = $0.75 R_\odot$). An estimate of the total viscous damping per period is one-third for the (1,1) mode. All other modes are damped more strongly. We can conclude the following if current models of the sun's envelope are realistic. When any transient disturbance excited r-modes in the CZ, the modes cannot retain their initial amplitudes for more than a few solar rotations without a fresh injection of energy at the proper phase (see Table 1.2 for damping rate).

One way to seek r-modes is to attempt direct detection of their horizontal motion. For this approach, it is best to go from a coordinate frame rotating with the sun to an inertial frame. In an inertial frame, the middle columns of Table 1.3 give the rotation rate and period of various modes, based on a convective zone rotating with a period of 25.7 days. Viewed from the frame rotating with the earth (synodic) at 365.3 days two rates may be of interest: the synodic rate and the repetition rate, at which phenomena caused by one r-mode repeats itself on the apparent solar disk. Table 1.3 shows the range of periods by listing the lowest and highest angular harmonics. The values for frequency and period apply to any surface feature varying linearly with displacement, such as velocity. Convection is likely to be modulated by r-modes. The overturning times of the large cells in the lower half of the convection zone are comparable to the oscillation periods of all r-modes with low l values.

Also the length scales of these deep seated cells are similar to those of r-modes with moderate l . Finally, convection has vorticity in the proper plane to couple with a toroidal velocity field. Thus the physical conditions for coupling are close to ideal. If convection is modulated on very large horizontal scales at time scales about one month, one should expect similar modulation in the various forms of solar activity like sunspots and flares. Wolff (1974) early suggested a relation between large scale convection and solar activity and since has provided additional observational material based on modes in the interior. Surface features would be affected more efficiently by the envelope r-modes, if they are indeed excited. This gives reason to search the solar observational record for evidence of

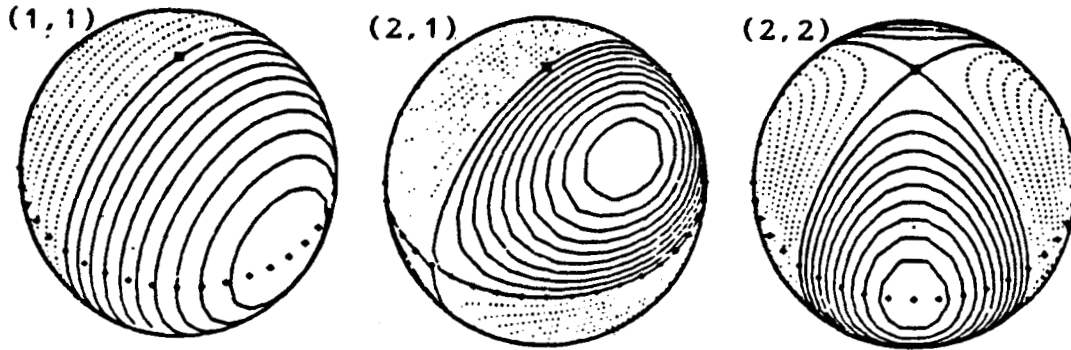


Fig. 1.1 Schematic fluid motion of r-modes with various values of l and m , near surface of the sun (after Saio, 1982).

Table 1.1 Spherical harmonic terms of the stress tensor for low order r-modes (after Wolff). r =radial dist; f =angular func(θ in eq 1.3)

D_{ij}	$l,m = (1,1)$	$(2,1)$	$(2,2)$
	$v_\theta = -rf\cos\theta$	$-rf\cos\theta\cos\theta$	$rf\sin\theta\cos(2\theta)$
	$v_\phi = rfcos\theta\sin\theta$	$rf\cos 2\theta\sin\theta$	$rf\sin 2\theta\sin 2\theta$
$D_{rr}=0$	0	0	0
$D_{\theta\theta} = \frac{2dv_\theta}{r d\theta}$	0	$+2f\sin\theta\cos\theta$	$-4f\cos\theta\cos 2\theta$
$D_{\phi\phi} = \frac{2}{r} \left(\frac{1}{\sin\theta} \frac{dv_\phi}{d\theta} + v_\phi \cot\theta \right)$	0	$-2f\sin\theta\cos\theta$	$+4f\cos\theta\cos 2\theta$
$D_{r\theta} = \frac{dv_\theta}{dr} - \frac{v_\theta}{r} = r \frac{d}{dr} \left(\frac{v_\theta}{r} \right)$	$-rf'\cos\theta$	$-rf'\cos\theta\cos\theta$	$rf'\sin\theta\cos 2\theta$
$D_{r\phi} = \frac{dv_\phi}{dr} - \frac{v_\phi}{r} = r \frac{d}{dr} \left(\frac{v_\phi}{r} \right)$	$+rf'\cos\theta\sin\theta$	$rf'\cos 2\theta\sin\theta$	$rf'\sin 2\theta\sin 2\theta$
$D_{\theta\theta} = \frac{1}{r} \left(\frac{1}{\sin\theta} \frac{dv_\theta}{d\theta} + \frac{dv_\theta}{d\theta} - \frac{dv_\theta}{d\theta} \cot\theta \right)$	0	$-f\sin 2\theta\sin\theta$	$2f(1+\cos^2\theta)\sin 2\theta$
$\frac{1}{2}(D_{ij})^2 =$	$2(rf')^2 \times (1-\sin^2\theta\sin^2\theta)$	$2(rf')^2 g_1(\theta, \theta) + 8f^2 \sin^2\theta g_2$	$8f^2 \{ 4\cos^2\theta + \sin^4\theta \sin^2 2\theta \} + 8(rf')^2 \sin^2\theta \times (1-\sin^2\theta\sin^2 2\theta)$

Table 1.2 Eigenfunctions (1,m,n) numerically calculated for 140 radial zones in the solar convection zone. E DOT=viscous energy change= E_v in eq. 1.3; K.E.=kinetic energy; SIGMA PRIME=damping rate.

EIGEN 1,1,0 -	E DOT	K.E.	SIGMA PRIME
	-----	-----	-----
	2.501470E+11	7.532208E+17	1.235631E-05
EIGEN 1,1,1 -	E DOT	K.E.	SIGMA PRIME
	-----	-----	-----
	2.955946E+14	6.574806E+20	3.480709E-05
EIGEN 1,1,2 -	E DOT	K.E.	SIGMA PRIME
	-----	-----	-----
	8.322445E+17	2.183930E+24	5.951347E-05
EIGEN 2,1,1 -	E DOT	K.E.	SIGMA PRIME
	-----	-----	-----
	9.838837E+11	6.747723E+17	2.300557E-04
EIGEN 2,1,2 -	E DOT	K.E.	SIGMA PRIME
	-----	-----	-----
	2.622679E+15	1.748582E+22	6.733799E-05
EIGEN 2,2,0 -	E DOT	K.E.	SIGMA PRIME
	-----	-----	-----
	4.828180E+11	3.826475E+18	1.040677E-05
EIGEN 2,2,1 -	E DOT	K.E.	SIGMA PRIME
	-----	-----	-----
	1.074537E+15	2.954031E+21	2.083029E-05
EIGEN 2,2,2 -	E DOT	K.E.	SIGMA PRIME
	-----	-----	-----
	2.597350E+18	8.662428E+24	2.922550E-05

modulations at the rotation rates, repetition rates and beat frequencies of envelope r-modes (in the CZ). To first order, the r-modes oscillate and rotate at rates independent of all solar interior conditions except for the rotation of the fluid in which they are embedded. Thus the r-mode rotation rates are as predictable as the g-modes. Each r-mode sequence is determined by a single free parameter: a mean rotation rate of the cavity in which the modes are trapped. This implies regular but complex behavior in solar characteristics modulated by the r-modes. In summary, some periods of r-modes have been tabulated. Viscous damping is strong and removes one-third or more of the mode energy each oscillation period.

Table 1.3. Sidereal rotation of r-modes in the convection zone and the repetition of identical flow fields as viewed from Earth (Wolff & Blizard, 1986).

l	m	ROTATION		REPETITION, ν_{lm}	
		Rate (nHz)	Period (days)	Rate (nHz)	Period (days)
1	1	0.	00	-31.7	-365.3
2	1	300.0	38.6	268.3	43.1
2	2	300.0	38.6	536.6	21.6
3	1	375.0	30.9	343.3	33.7
3	2	375.0	30.9	686.6	16.9
3	3	375.0	30.9	1030.	11.2
00	1	450.0	25.7	418.3	27.7
00	2	450.0	25.7	836.6	13.8

2.1 FAST FOURIER TRANSFORMS OF THE ZURICH DAILY SUNSPOT NUMBER AND GREENWICH DAILY WHOLE SPOT AREA

A fast Fourier transform (FFT) of daily Zurich sunspot number was made for eight sets of data, taken near peaks of solar cycles 14-21. The FFT accepts 2048 bits of data, so 2048 days were included, starting with 1 Jan except for the most recent cycle, when the data set began 16 Nov 1978, when data was available from the ACRIM irradiance satellite experiment.

Thus the eight files contained 2048 days each, with a starting date of:

File 1	16 Nov 1978	File 5	01 Jan 1935
File 2	01 Jan 1966	File 6	01 Jan 1925
File 3	01 Jan 1956	File 7	01 Jan 1915
File 4	01 Jan 1945	File 8	01 Jan 1904

For a sequence of 2048 days, the FFT will display periods between 2 days and 1024 days (2.8 yrs) due to the pairing of the data. Prominent in most of the spectra is the 27-day peak. Periods longer than 160 days would not be resolved.

The Greenwich Photoheliographic Results, 1874-1981, (GPR), were obtained on magnetic tape from the National Geophysical Data Center of NOAA. In addition, an updated version of GPR 1982-1984 was obtained from Douglas Hoyt of NCAR. The GPR tape was loaded onto a VAX and pertinent columns extracted (date, whole spot area). A program was written to average data over four days. Another program was written to fill in zeros of whole spot area (when no observations were made), by averaging the values of the day before and day after. Because of large data gaps in early years, the period 1904-1984 was selected for study with fast Fourier transform (FFT) (Fig. 2.0).

FFTs were run on eight data sets with the same starting dates as for the Zurich sunspot number. In this case, the plots were on a single frame, rather than four frames for the previous data sets, since there were 512 points rather than 2048 (4-day averages) (Figs. 2.1-2.4). The mean of the eight spectra showed very little detail. For the 4-day averages, the limits on the FFT are 8 days and 5.6 years, but in practise the lower limit is 16 days because of the mirror image form of the Grafplot. Because the four-day smoothing resulted in improved spectra, it was applied to the Zurich sunspot number data, which were replotted (Figs. 2.5-2.8).

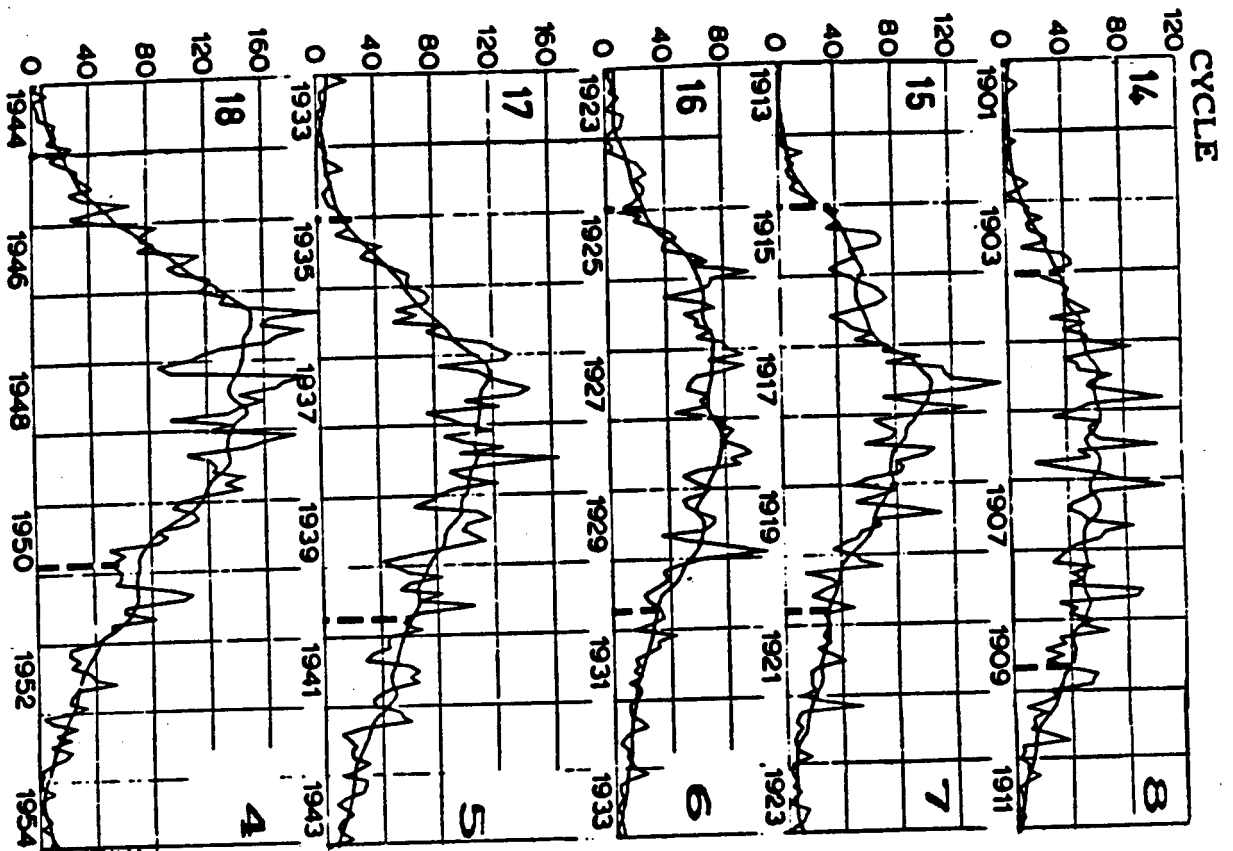
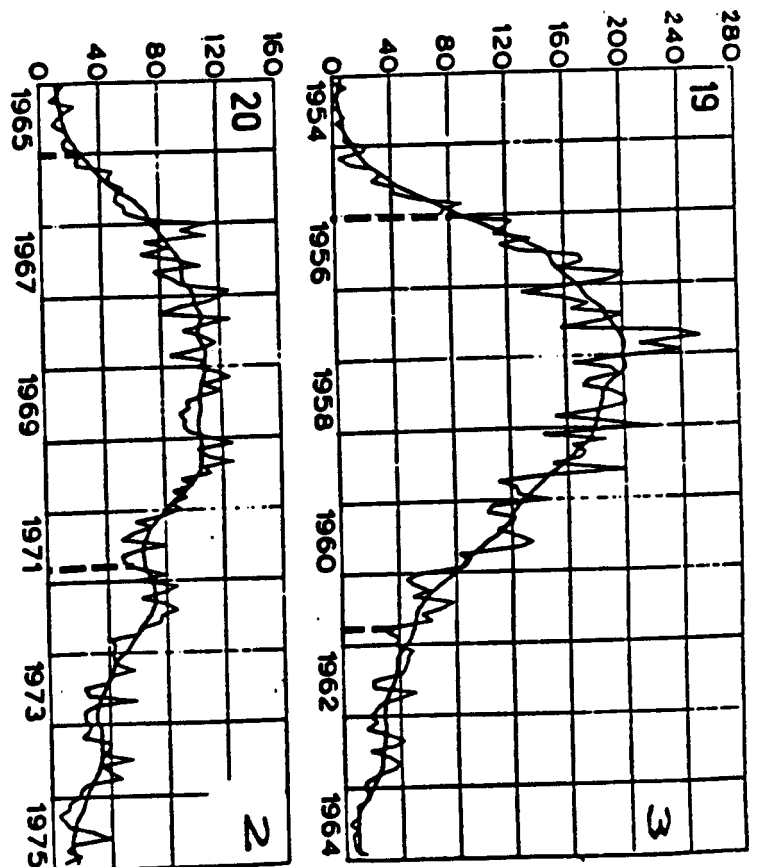


Fig. 2.0 20th century sunspot cycles. showing 5.6 yr samples (between dashed lines). Samples began on Jan 1 except for cycle 21, when dates corresponded to availability of ACRIM data.



ORIGINAL PAGE IS
OF POOR QUALITY

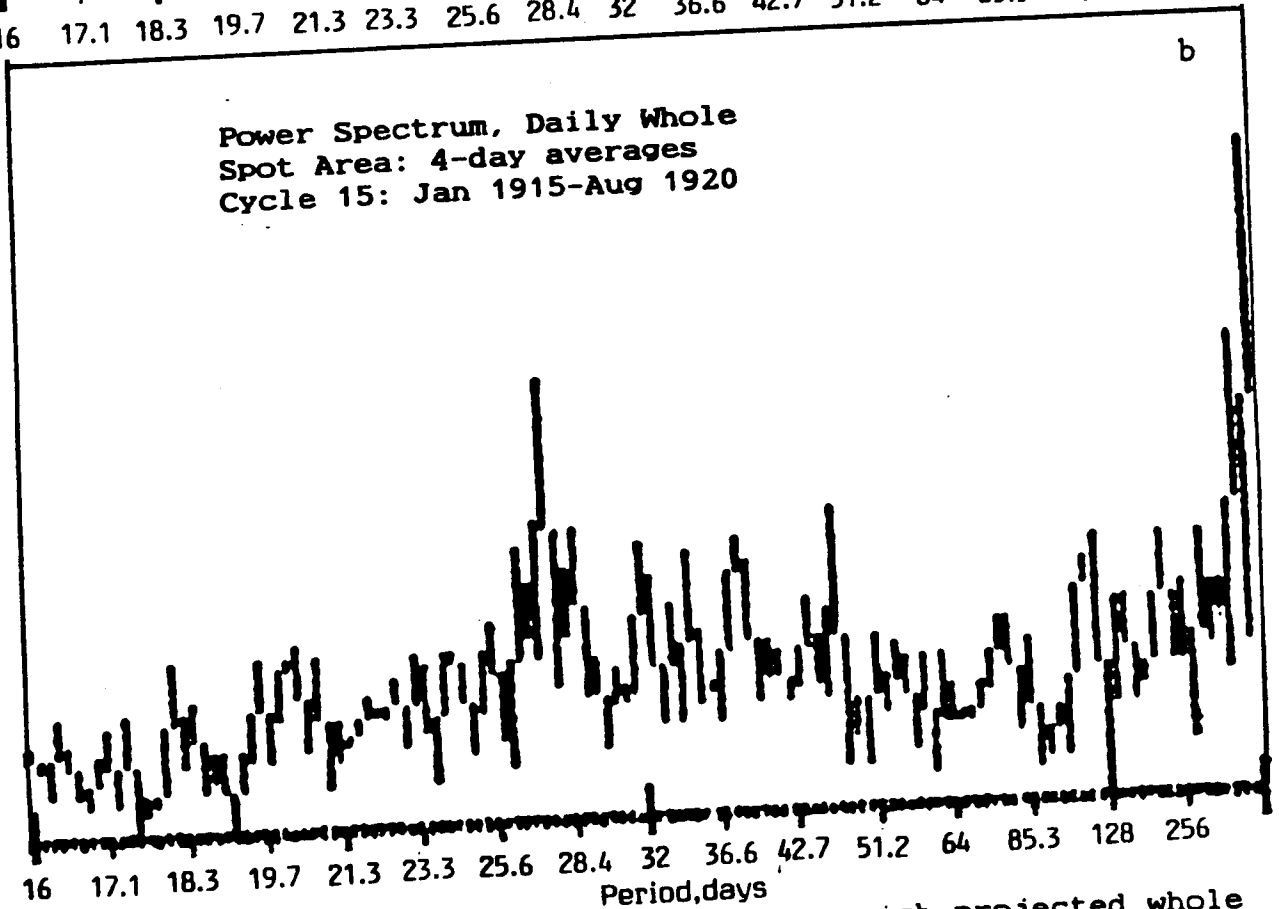
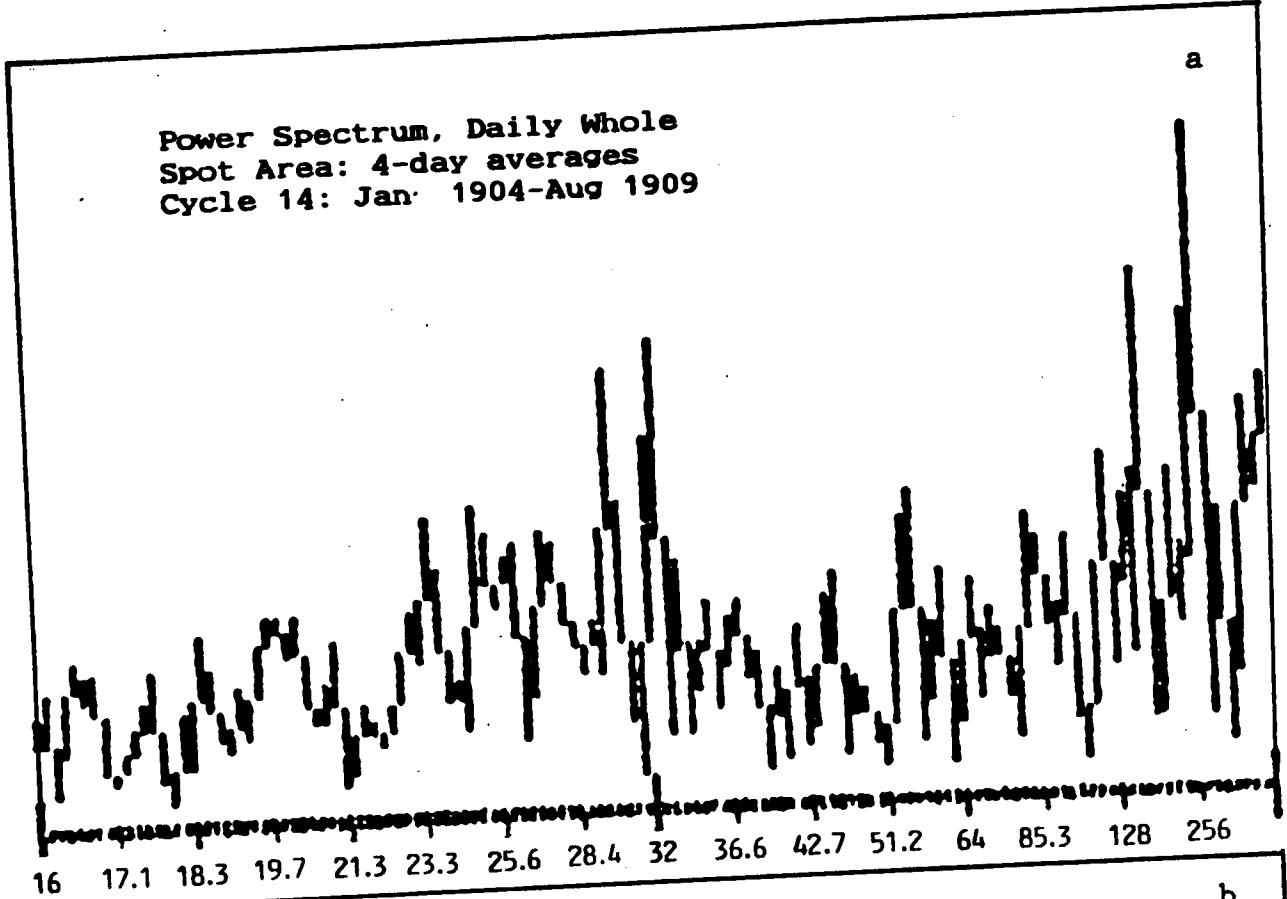


Fig. 2.1 Fast Fourier transforms of Greenwich projected whole spot area (4-day averages): cycles 14 and 15(a,b).

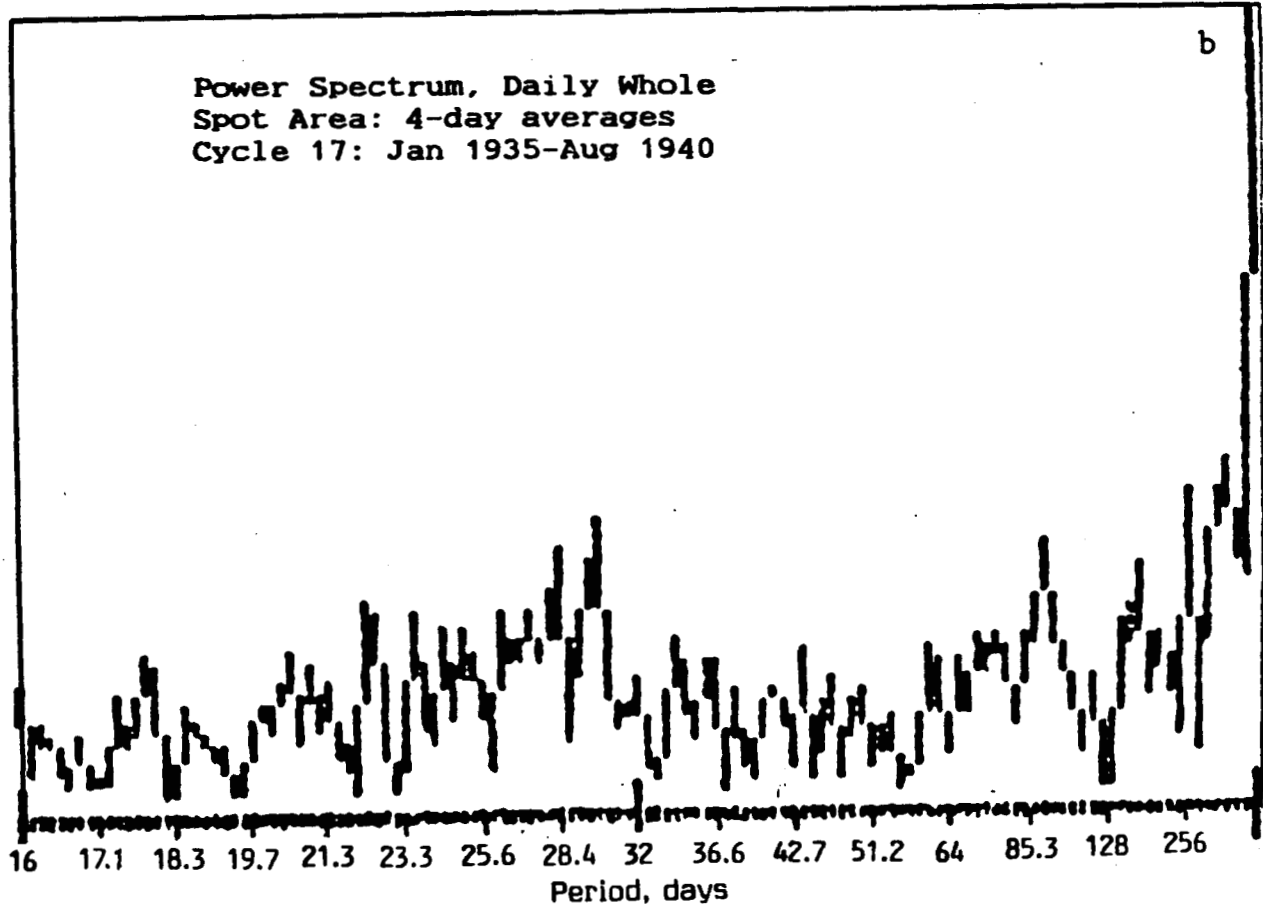
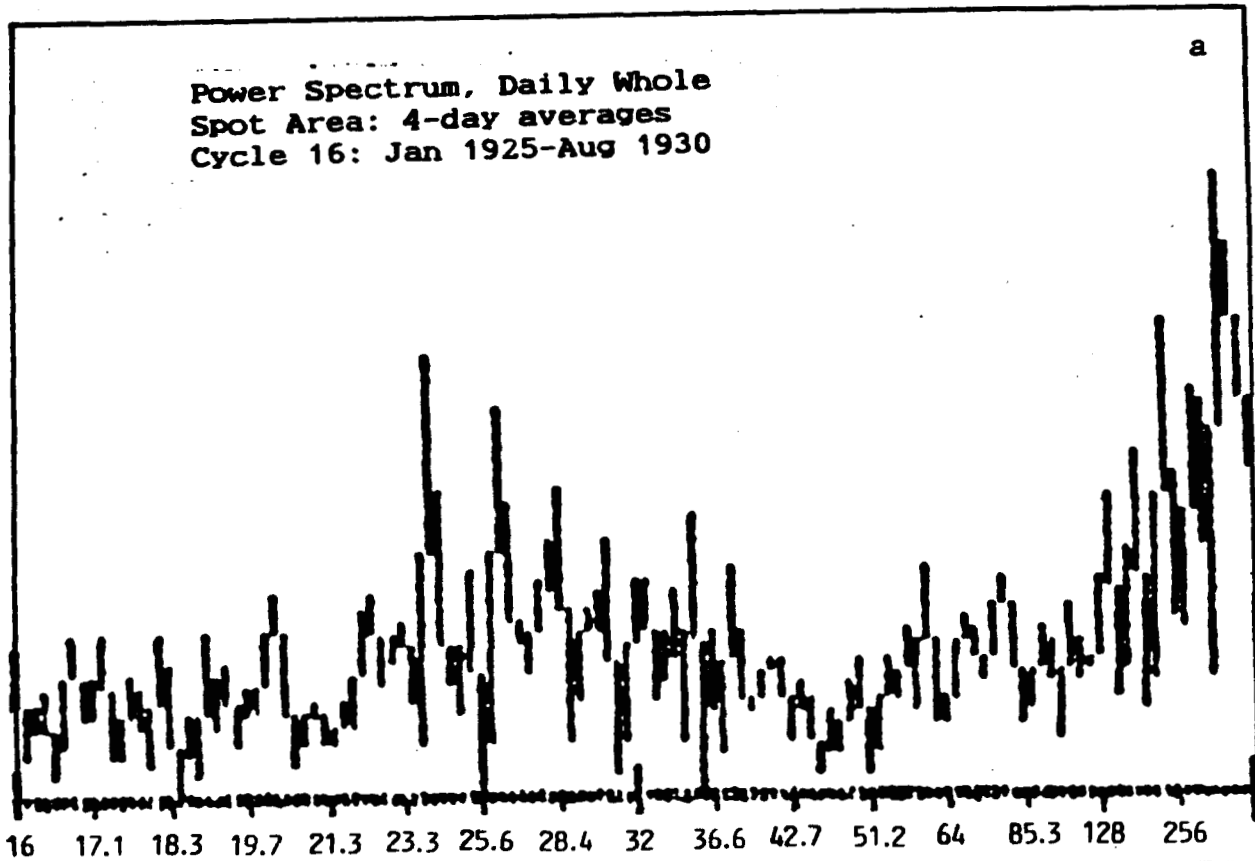


Fig. 2.2 Fast Fourier transforms of Greenwich projected whole spot area (4-day averages): solar cycles 16 and 17(a, b).

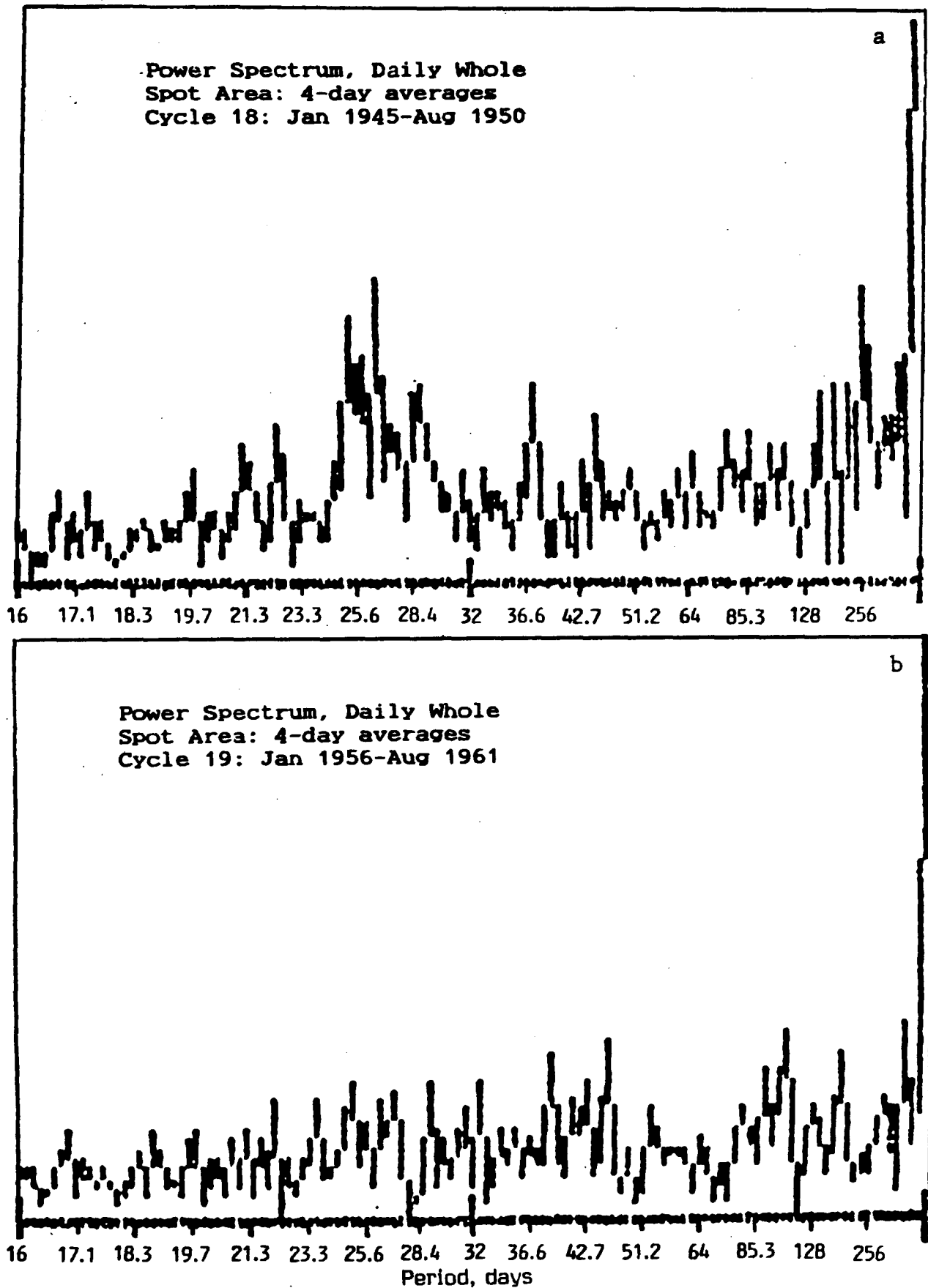


Fig. 2.3 Fast Fourier transforms of Greenwich projected whole spot area (4-day averages): solar cycles 18 and 19(a,b).

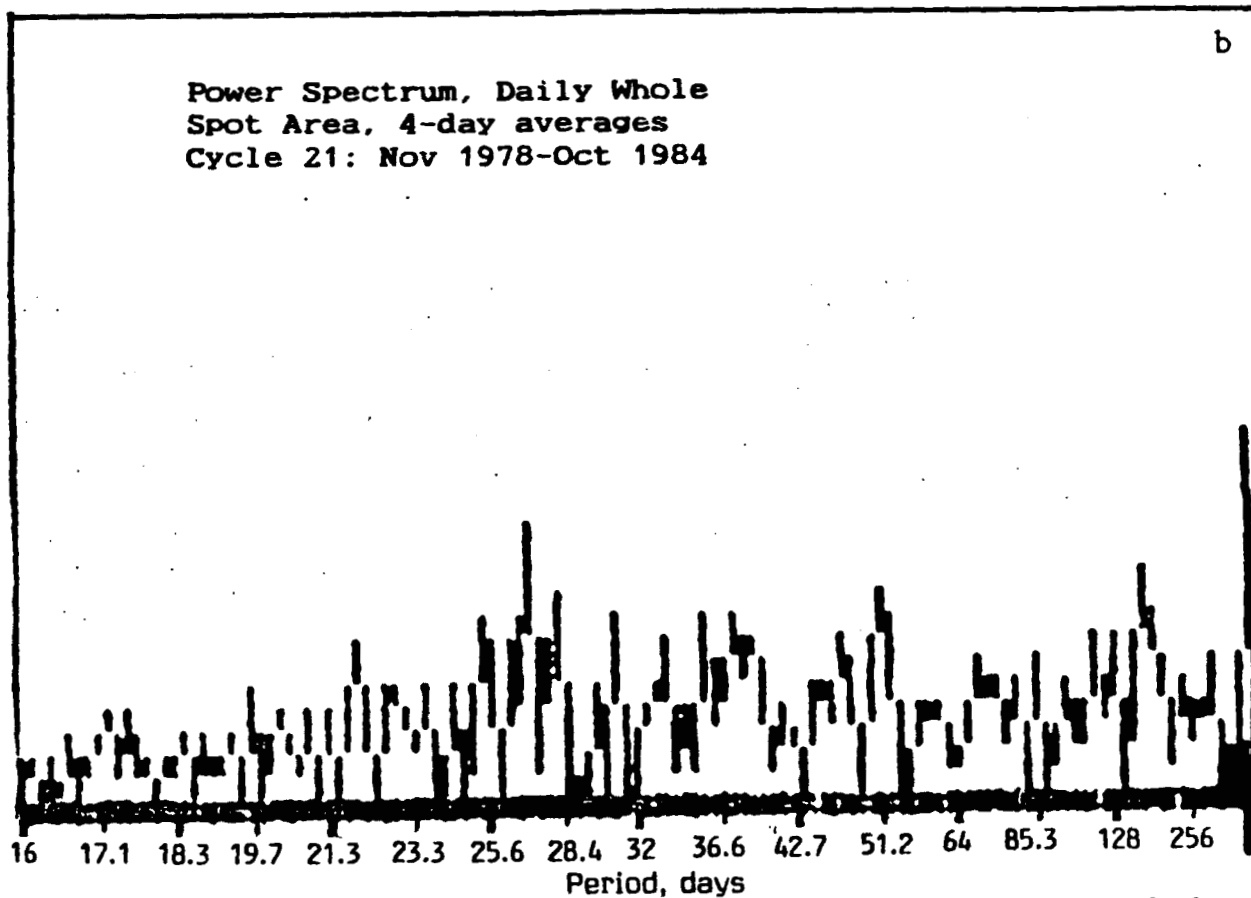
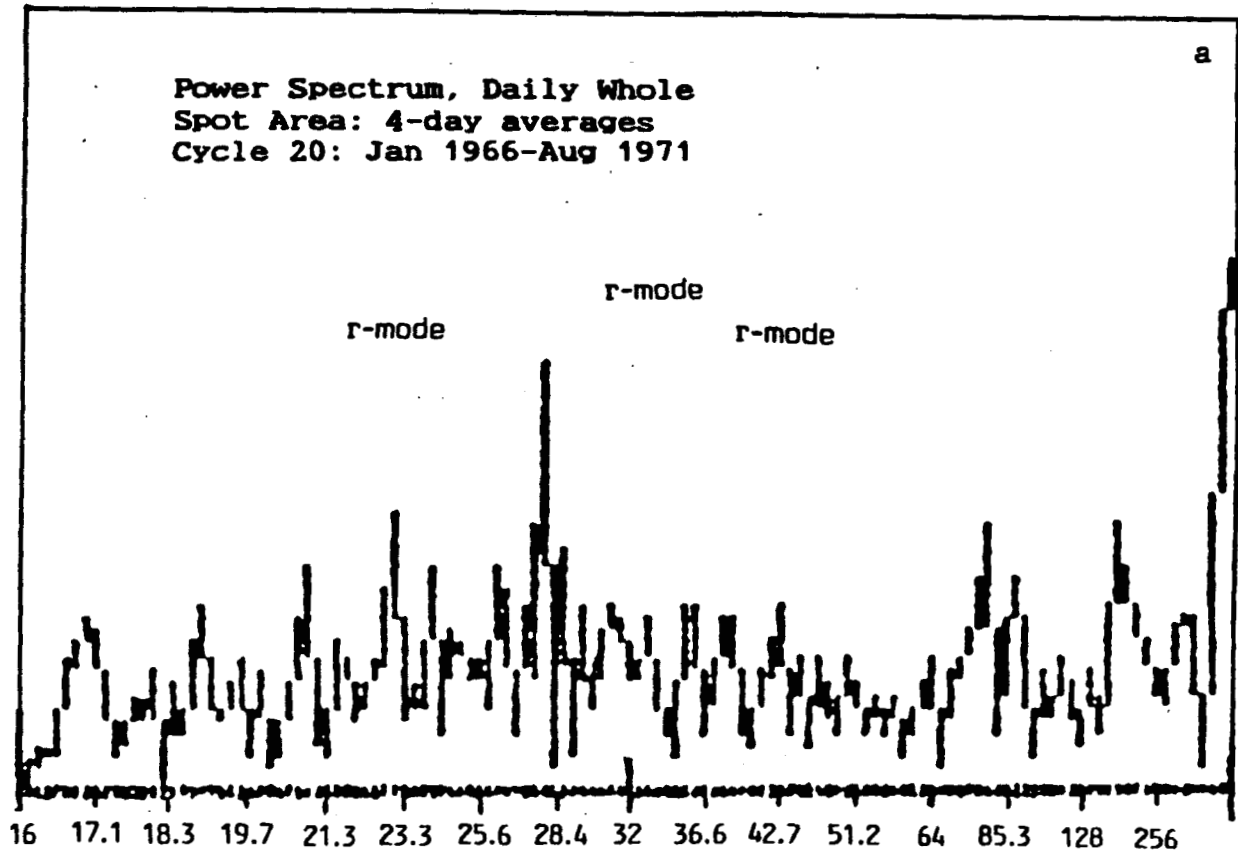


Fig. 2.4 Fast Fourier transforms of Greenwich projected whole spot area (4-day averages): solar cycles 20 and 21 (a, b).

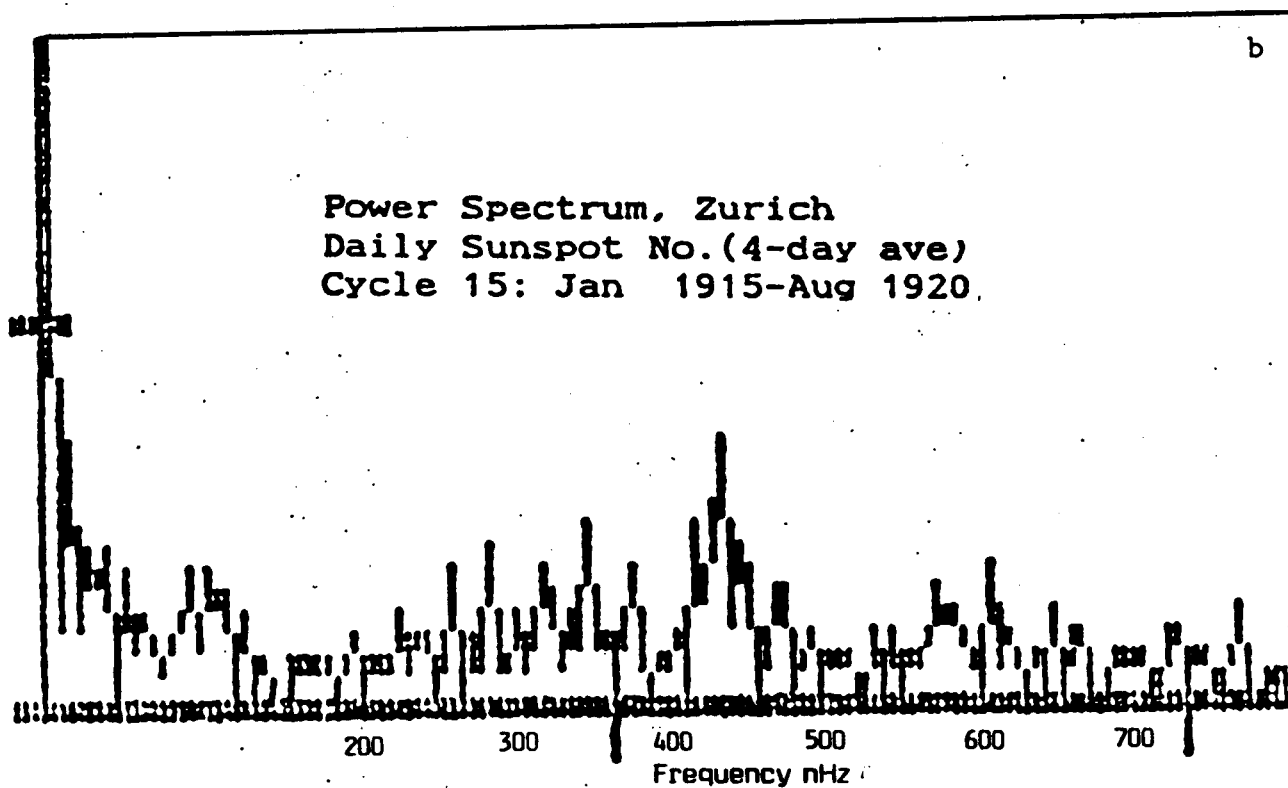
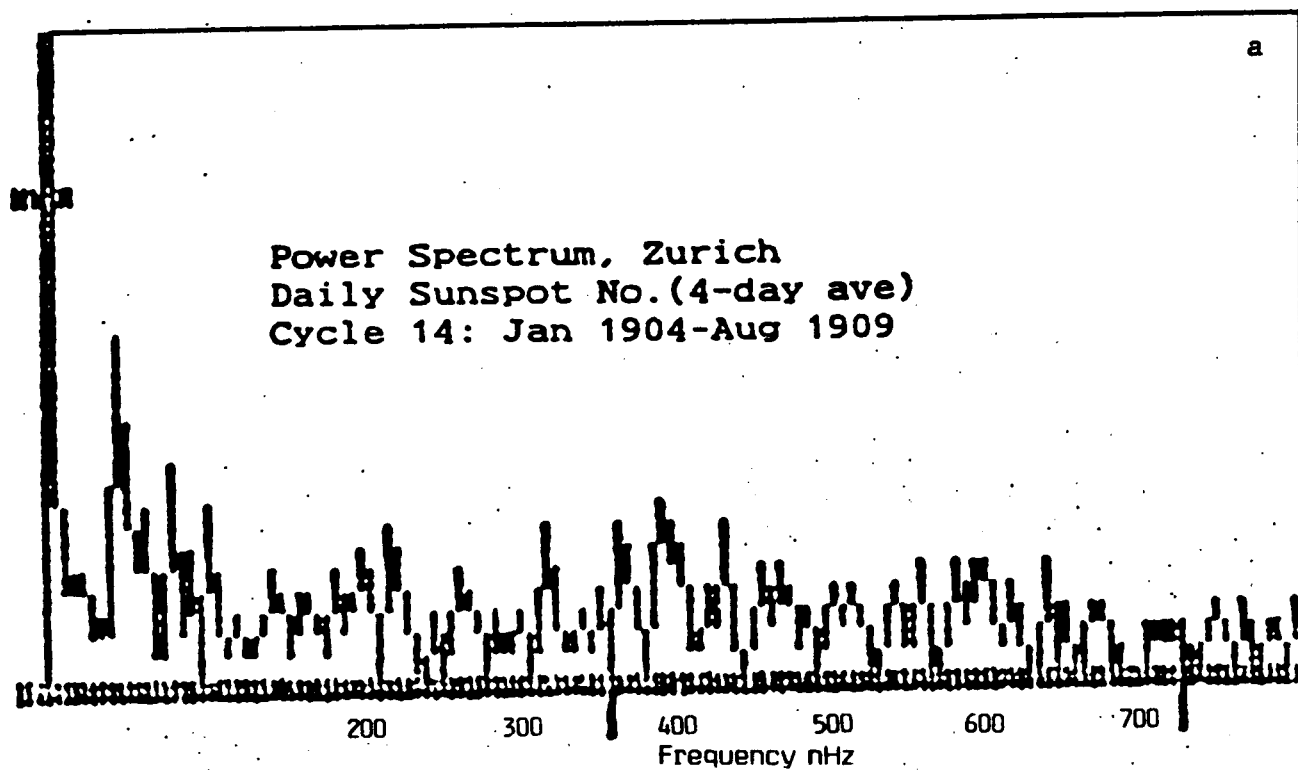


Fig. 2.5. Fast Fourier transforms of Zurich daily sunspot number (4-day averages) for solar cycle 14 (a) and 15 (b).

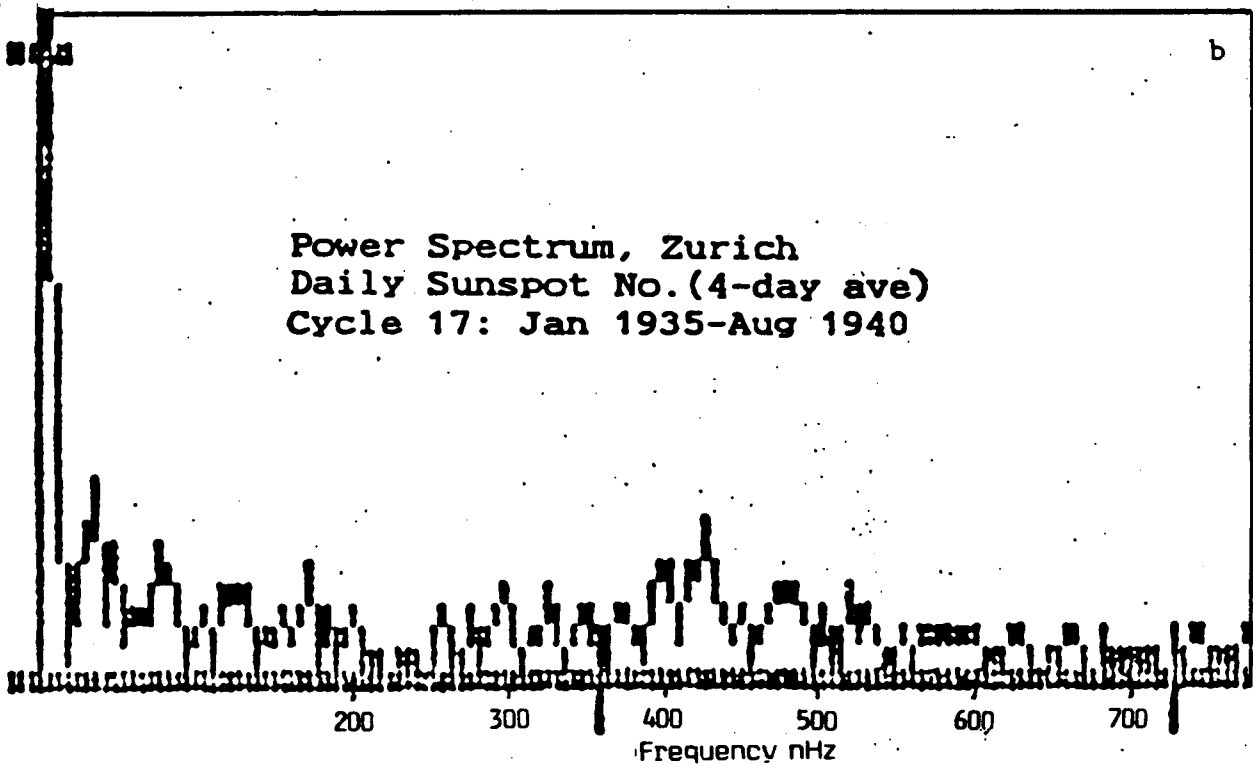
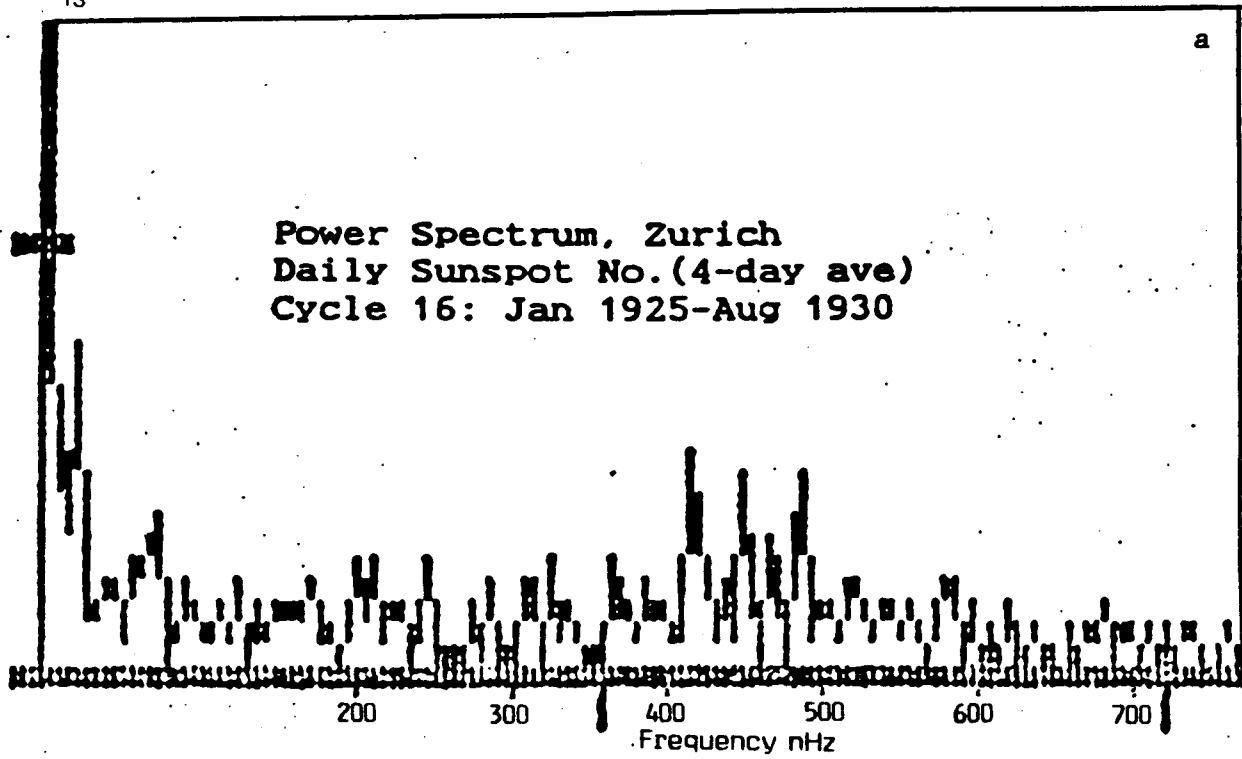


Fig. 2.6. Fast Fourier transforms of Zurich daily sunspot number (4-day averages) for solar cycle 16 (a) and 17 (b).

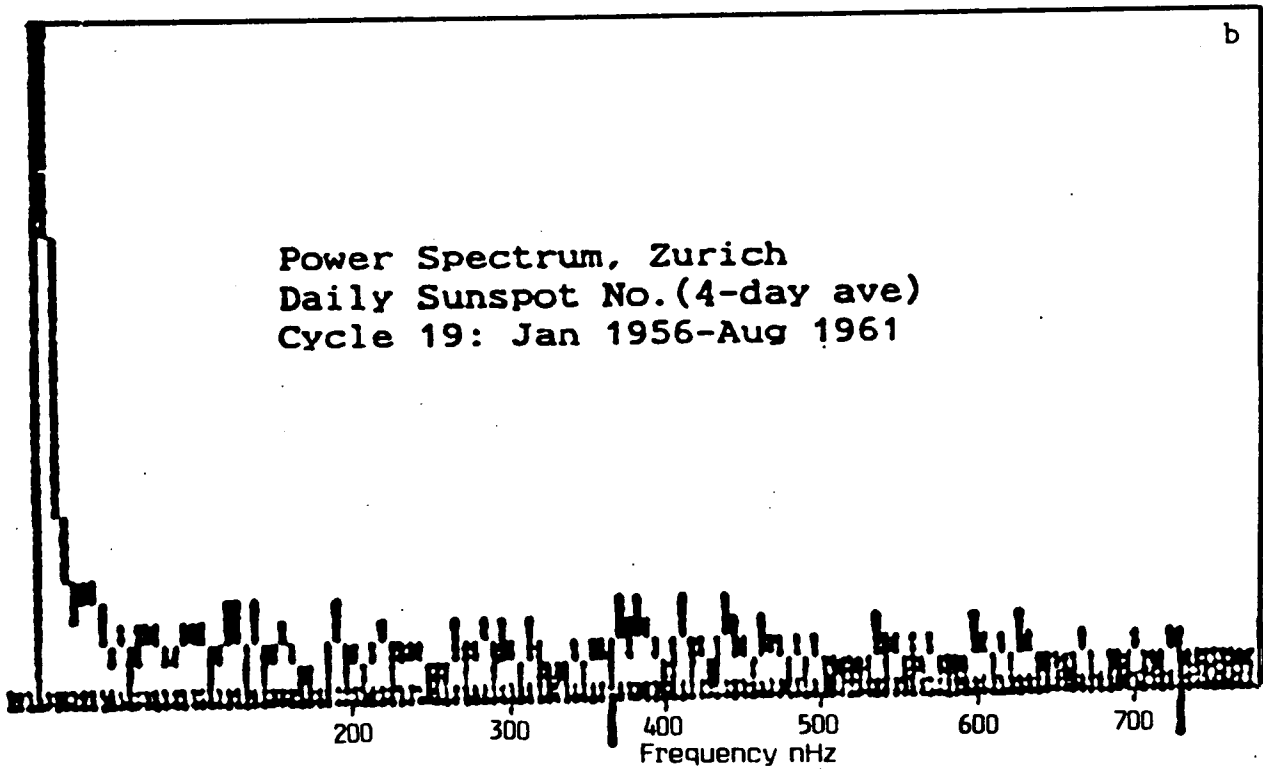
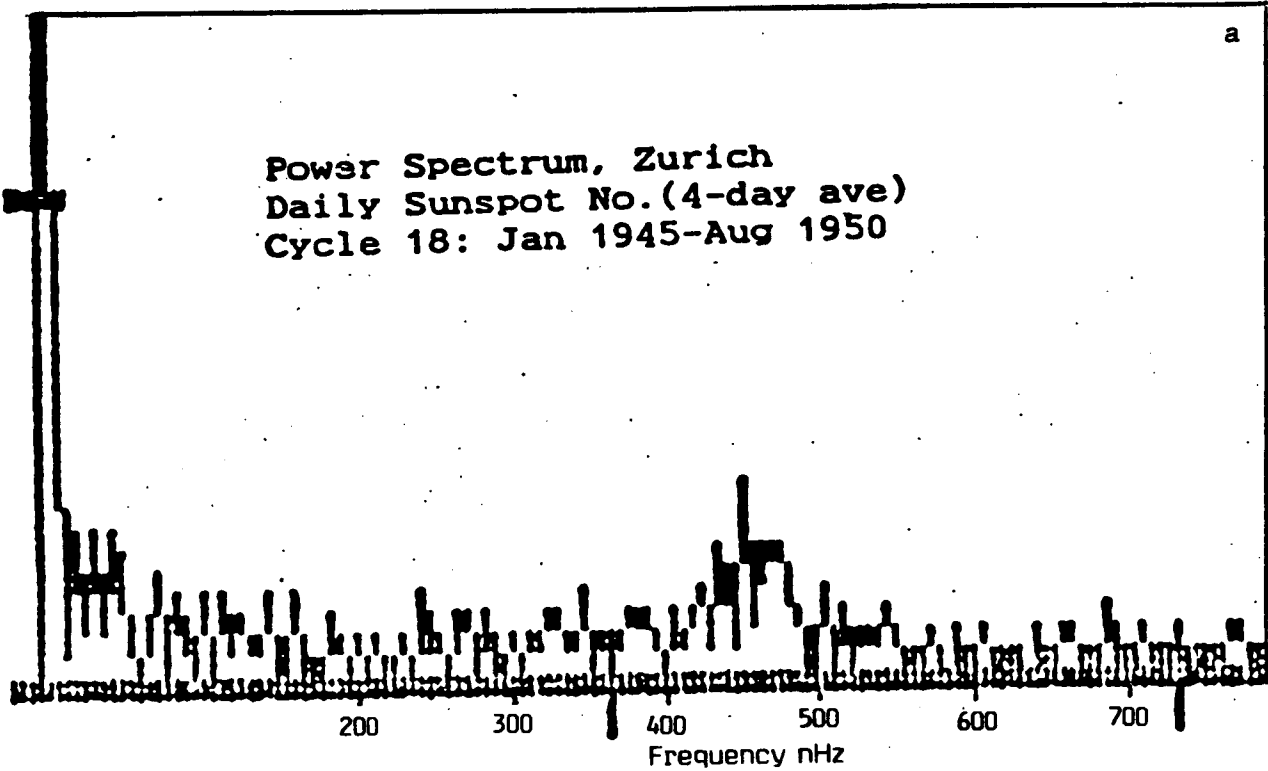


Fig. 2.7. Fast Fourier transforms of Zurich daily sunspot number (4-day averages) for solar cycle 18 (a) and 19 (b).

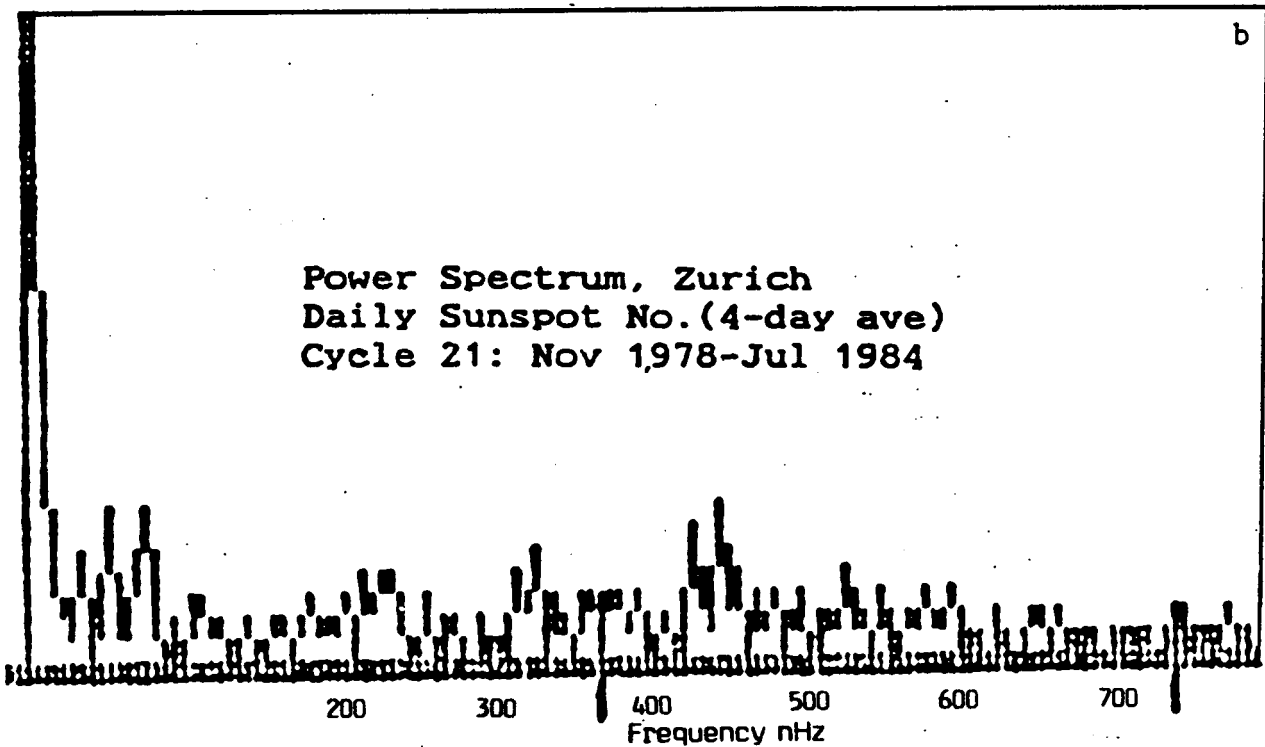
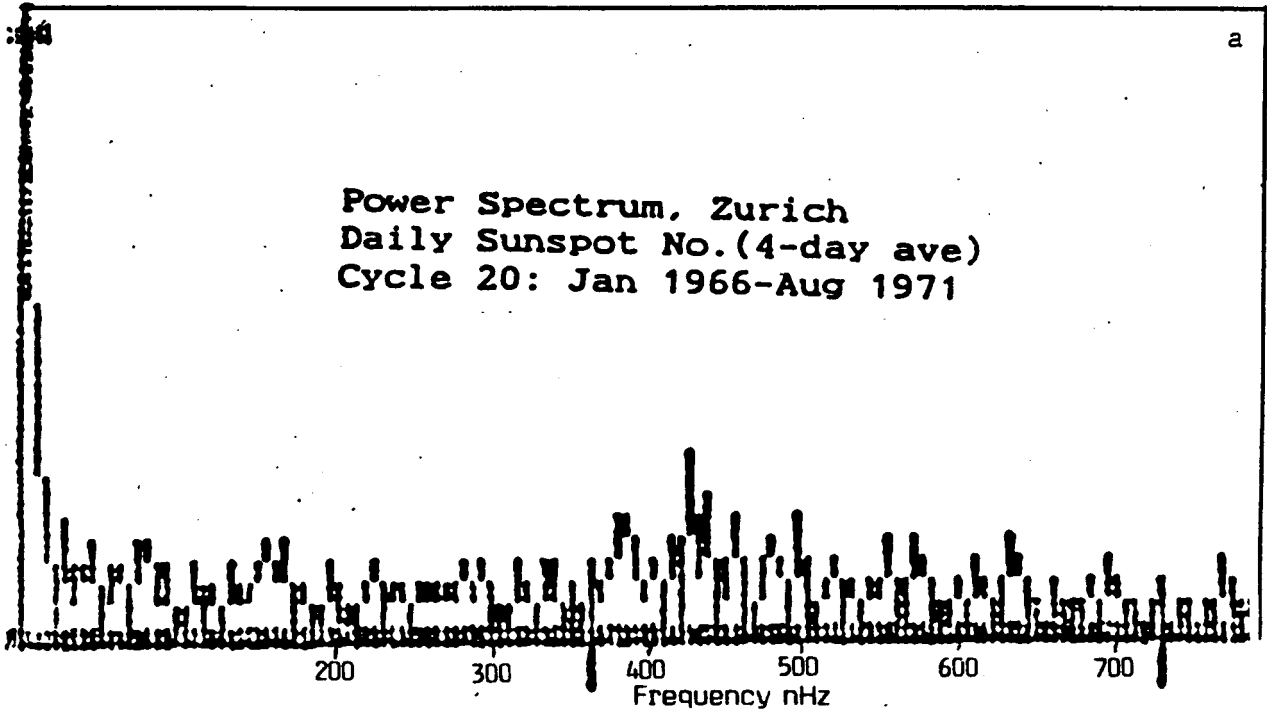


Fig. 2.8. Fast Fourier transforms of Zurich daily sunspot number (4-day averages) for solar cycle 20 (a) and 21 (b).

3 EVALUATION OF FFT'S WITH WOLFF & HICKEY (1987) MODEL

Each theoretical frequency having measurable power which stands out prominently in any spectra is listed in Table 3.1. Frequencies prominent in the earlier cycles were primarily caused by r-modes. Only one of the 7 cases where a line was clearly more prominent in the earlier cycles did not involve r-modes; 5 of the 7 were exclusively caused by r-modes. A different situation was found in the last cycle (21) (later in the solar cycle), where only 2 of the 8 cases did not involve g-modes. This is consistent with decaying r-modes which would be expected in the Sun. Wolff and Blizard (1986) found that turbulent viscosity would damp r-modes in a few months, and postulated that they might be excited irregularly by large convection events. Occasional injections of fresh energy would prolong r-mode oscillations. In any case, the above measurement showed r-modes to be a stronger influence in the first few years of solar cycles rather than later in the cycle, when their lessened influence allowed the presumably more stable g-modes to have relative prominence (see Fig. 2.0 & 3.1).

Figure 3.1 shows a Fourier spectrum of projected sunspot area (four-day averages). Below it lies the model lines from Wolff & Hickey (1987) and Table 3.1. The region between zero and 50 nHz contains many theoretical lines due to high-l modes, indicated here only as a group (labeled H). The data is unresolved but the high power measured there is expected. At frequencies above 50 nHz, there is a remarkable similarity between theory and the observed sunspot area spectra. Predicted lines occur where there is much observed power and minima in power tend to lie where there are no theoretical lines. All four of the prominent power maxima near 310, 380, 450 and 530 nHz are associated with the lowest angular harmonic. The first three correspond to beats involving the $l=1$ r-mode. The fourth involves the $l=1$ g-mode and the feature H. This supports the expectation that the lowest modes are the most influential on variations of sunspot area (and other indicators of solar activity).

Only three peaks (100, 170 and 295 nHz) occur near no predicted line. Finally, considerable power is seen in the 7 bands which all arise from feature H. All seven lie where there is considerable observed power and 5 of the 7 include observed maxima. If the model is correct, it implies that the combined effect of all high harmonic r-modes can be comparable to one low harmonic in modulating sunspot area. Overall, the agreement seen in Table 3.1 and Figure 3.1 is much better than one could expect by chance, since there were effectively fewer than two free parameters to adjust the 28 model frequencies (Wolff & Hickey, 1987).

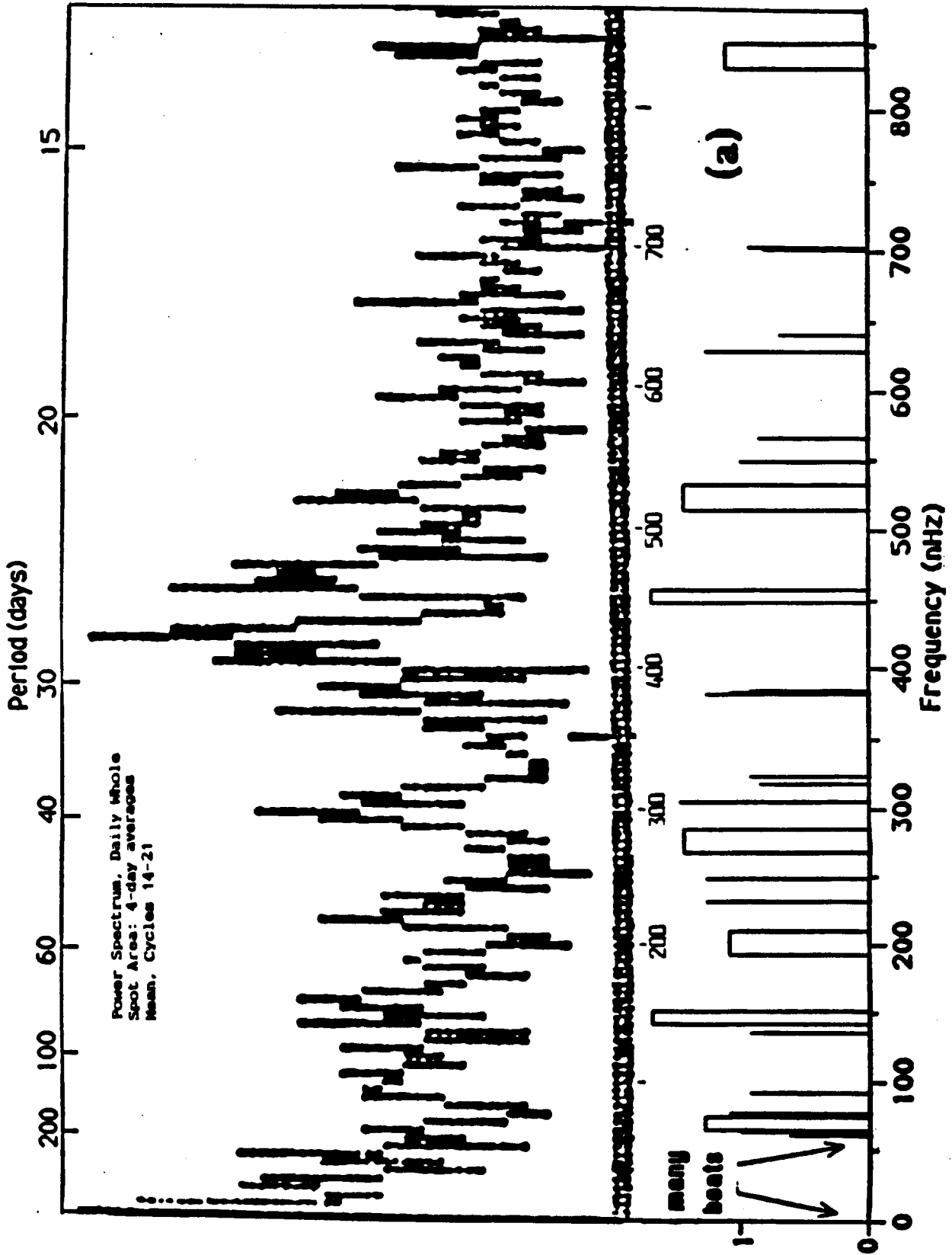


Fig. 3.1. (Top) Mean Fourier spectrum of solar cycles 14-21, daily projected whole spot area (4-day averages). (Below) Model lines and bands from Wolff & Hickey (1987).

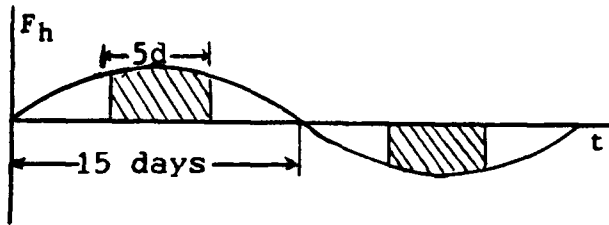


Fig. 4.1. Duration of F_h over 5 d period during 15 d. half-cycle.

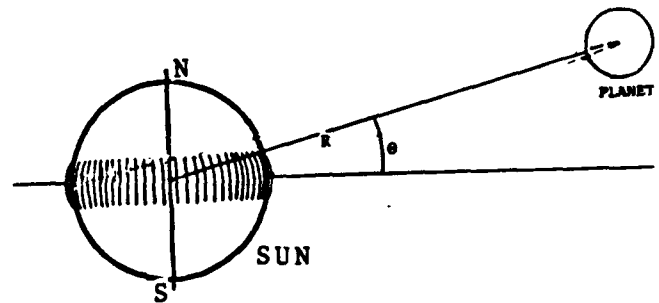


Fig. 4.2. Torque exerted on equatorial bulge by a planet.

4.1 MAGNITUDE OF EXTERNAL TORQUE

We wish to calculate if the horizontal component F_h of the force exerted by a planetary torque, does work on the photospheric layers at a rate comparable to $10^{-6} L_{\odot}$ (the mean rate of energy seen released by solar activity). Assume that F_h is constant and acts for about 5 days (1/6 rotation of the sun) on a volume element of the photosphere, accelerating it away from the equator with no resisting force (for simplicity)(Fig. 4.1). Then the horizontal velocity is $v_h = (F_h)t$, where F_h is in units of force/mass, then (kinetic energy/volume) = $1/2 \rho v_h^2$. In choosing ρ , we do not go into the convecting interior because these layers may have a stiffness that resists the torque-induced flow, since they experience strong horizontal diffusion of momentum. This would give an upper limit to an energy source fed into the photosphere. The long-term mean rate of energy deposition would be:

$$\frac{(\text{vol. equatorial bulge in photosphere}) \times \rho / 2 [v_h(\text{for } t=5 \text{ days})]^2}{15 \text{ days}}$$

The force of an external body on the sun may be calculated from McCullagh's formula, which expresses the gravitational potential of any body at a distance R and with a mass M (see section 3.1):

$$V = GM/R + GM(A+B+C-3I)/2R^3 + \text{higher order terms} \quad (4.1.1)$$

where A , B and C are the principal moments of inertia of the Sun. It is usual to write $J_2 = 3/2(A-C)/MR_{\odot}^2$, where J_2 is the quadrupole moment. Since we assume that the sun is axisymmetric, to a first approximation, $A=B$, and $(A-C)/C$ is approximately 10^{-5} (Hill, 1975). The torque of an external body is obtained by finding the force from the above equation (4.1.1) by differentiation; since the first term vanishes, the torque is then $F_x R$, or, (see Fig. 4.2 for $\sin \theta$),

$$\Gamma = 3GM(A-C)\sin \theta / R^3 \quad (4.1.2)$$

Using $I_{\odot} = 3 \times 10^{46} \text{ kg-m}^2$, and $G = 6.67 \times 10^{-11} \text{ m}^2/\text{kg}^2$,

$$\Gamma = 36.67 \times 10^{-11} \text{ Nm}^2/\text{kg}^2 (3 \times 10^{46} \text{ kg-m}^2) (10^{-5}) M_j \sin \theta / R^3 \quad (4.1.3)$$

Substituting for Jupiter, $M_j = 19.1 \times 10^{27} \text{ kg}$, $R_j = 7.78 \times 10^{11} \text{ m}$, and

$\sin 6^\circ = 0.104$, then the torque due to Jupiter is $= 24.0 \times 10^{24} \text{ N-m}$ (Joules). For other planets, $p = 20.0 \times 10^{16} \text{ n-m}^2/\text{kg}^2 (M_p \sin \theta / R_p^3)$.

.. Next, calculate the volume V_b of the oblate equatorial belt of the Sun:

$$V_b = (2\pi R_\odot) \Delta R \Delta H \quad (4.1.4)$$

where $\Delta R/R_\odot = 10^{-5}$ and, arbitrarily, $\Delta H = 2 \times 10^8 \text{ m}$, then

$$V_b = 6.2 \times 10^{21} \text{ m}^3 \quad (4.1.5)$$

Now, find the mass of the oblate belt, using a density for the photosphere $\rho = 3 \times 10^{-5} \text{ kg/m}^3$ (Abell, 3rd Ed). Then,

$$M_b = \rho V_b = 18.6 \times 10^{16} \text{ kg} \quad (4.1.6)$$

Consider the torque from one planet, say, Jupiter (equation 4.1.3 and so on). Find the average horizontal force from the quadrupole term,

$$F_h = \Gamma_j / R_\odot = (24.0 \times 10^{24} \text{ N-m}) / 7.0 \times 10^8 \text{ m} = 3.42 \times 10^{16} \text{ N} \quad (4.1.7)$$

Calculate the horizontal velocity $v_h = (F_h)t$, where $t = 5$ days, and F_h is the force per unit mass (divide by mass of belt, M_b):

$$v_h = F_h / M_b (5 \text{ days}) = 79.4 \text{ km/s} = 7.94 \times 10^4 \text{ m/s} \quad (4.1.8)$$

which is the same order of magnitude as the equatorial velocity of the sun, equal to 2 km/sec.

Now calculate the kinetic energy per unit time,

$$\begin{aligned} (\text{KE/sec}) &= V_b \times (1/2) \rho (v_h)^2 / 15 \text{ days} \\ &= 45.2 \times 10^{19} \text{ N-m/s} = 45.2 \times 10^{19} \text{ J/s} \end{aligned} \quad (4.1.9)$$

Compare this figure to the energy of solar activity, $10^{-6} L_\odot$, which is $4 \times 10^{20} \text{ J/sec}$ (Allen, 1973). Thus,

$$\begin{aligned} (\text{KE/sec}) &= 45.2 \times 10^{19} \text{ J/s} > (10^{-6}) (4 \times 10^{20} \text{ J/s}) \\ (\text{KE/sec}) &> 10^{-6} L_\odot \end{aligned} \quad (4.1.10)$$

So the energy input is much greater than the estimated energy of solar activity.

4.2 TIME SPAN OF TORQUE IN EXTERNAL SECTOR OF SUN

For the case of two planets, the problem is to find how long both planets are located in a sector of given angular width as viewed from the sun, near heliographic conjunction. Analytically, one uses angular velocity, w , or the equivalent, $2\pi/P$, where P is the planet period in convenient units, such as days. Then start from the two innermost planets and proceed outwards. Let t be the time both Mercury and Venus are located in a given sector of heliocentric longitude, θ , then,

$$\Delta\theta = (\Delta w)t \quad \text{so } t = \Delta\theta/\Delta w = \Delta\theta/(w_1 - w_2) \quad (4.2.1)$$

or using periods,

$$t = \Delta\theta/2\pi(P_1P_2)/(P_2 - P_1) \quad (4.2.2)$$

when angles are expressed in radians. If the angles are in degrees, multiply by $360^\circ/2\pi$. If one uses an angular sector of $1/2$ radian (28.65°), then the time in equation (4.3.2) becomes

$$t = \frac{1}{4\pi} \frac{(87.969 \text{ d})(224.70 \text{ d})}{(224.701 - 87.969)\text{d}} \approx 11.50 \text{ days} \quad (4.2.3)$$

Similarly for all other combinations of two planets. Using sidereal periods in days (Allen, 1973) one obtains the values in Table 4.1 A graph can be used to check results. Find the degrees/day each planet moves in longitude (Astron. Almanac) and plot on a solar system chart. Diagram the time taken for a given planet to move 28.65° in heliocentric longitude, and compare with another planet when they are in conjunction (see Fig. 4.2.1, Tables 4.1 & 4.2).

The axial rotation of the sun does not enter here. Using the axial angular velocity of the sun, w_\odot , and the two planetary revolutionary velocities, w_1 & w_2 , it can be shown that w_\odot cancels out (where w_1' and w_2' are synodic velocities):

$$\begin{aligned} \Delta w &= w_1' - w_2' & \text{but } w_1' &= w_\odot - w_1 \\ \text{so,} & & & \\ \Delta w &= (w_\odot - w_1) - (w_\odot - w_2) = w_1 - w_2 \end{aligned} \quad (4.2.4)$$

Table 4.3 shows the "synodic" periods of the planets as viewed from the subsolar point on the sun's surface.

Finally, Table 4.4 lists the relative amplitude of precessional torque of the various planets.

ORIGINAL PAGE IS
OF POOR QUALITY

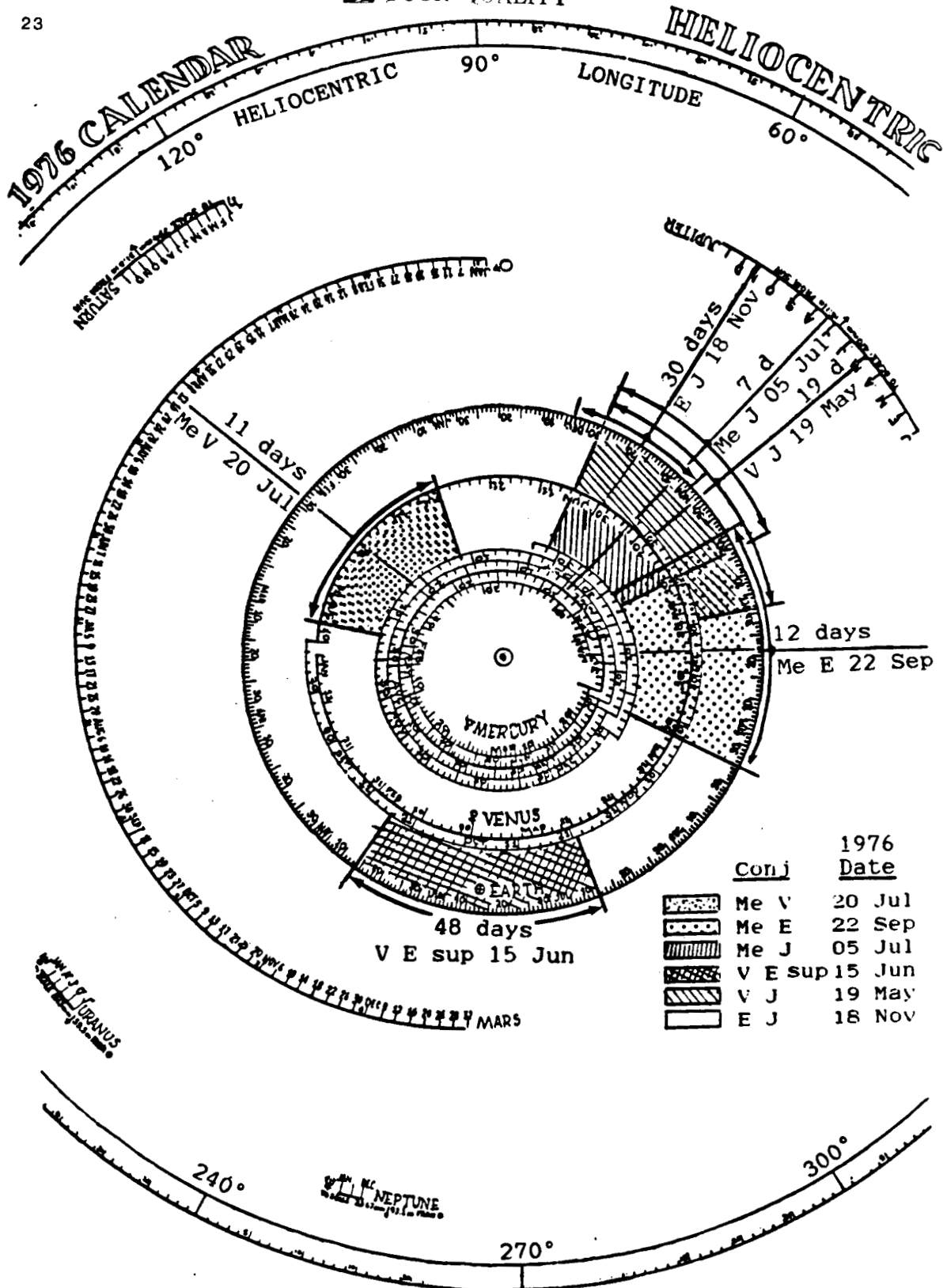


Fig.4.2.1. Plan view of solar system, showing planet positions by 1976 date. Time span when 2 planets are within a sector of half radian near conjunction.

ORIGINAL PAGE IS
OF POOR QUALITY

Table 4.1 Days that two given planets are within a sector of $\frac{1}{2}$ radian viewed from the sun. (Allen, 1973).

	P(days)*	Venus	Earth	Mars	Jupiter	Saturn	Uranus	Neptune
Mer	87.969	11.504	9.221	8.028	7.145	7.06	7.02	7.01
Ven	224.701		46.47	26.572	18.86	18.26	18.01	17.9
Ear	365.256			62.065	31.74	30.09	29.42	29.2
Mars	686.780				64.95	58.40	55.92	55.3
Jup	4332.589					577.21	401.46	371.5
Sat	10759.22						1318.50	1042.6
Ura	30685.4							4834.1
Nep	60189.							

* sidereal

Table 4.2 Days that two planets are within $\frac{1}{2}$ radian, heliocentric longitude, viewed from the sun; four solutions (Astron Almanac)

1976 dates	Conj Planets	days				deg/day
		Calc.	Graph	P'/4T	Daily M	
20 Jul	Me V	11.5	11.0	11.5	7.78	5.28-1.6°
22 Sep	Me E	9.22	11.5	9.21	8.32	4.44-1.0°
05 Jul	Me J	7.15	9.0	7.15	4.83	6.06-0.09°
15 Jun*	V E	46.5	44.0	46.5	46.2	1.62-1.0°
19 May	V J	18.9	20.0	22.4	18.9	1.60-0.09°
18 Nov	E J	31.7	30.5	31.8	31.5	1.00-0.09°

*superior conjunction

Table 4.3. Periods of the planets, viewed from the subsolar point. The sidereal rotation period of the sun is taken as 25.80 days (Wolff, 1976). (Allen, 1973)

	Sidereal Period	Synodic Period
Mercury	87.969 d	36.51 d
Venus	224.701	29.15
Earth	365.256	27.76
Mars	686.790	26.81
Jupiter	4332.589	25.95
Saturn	10759.22	25.86
Uranus	30685.4	25.82
Neptune	60189.	25.81

Table 4.4 Relative amplitude of precessional torque of planets on the sun. (Allen, 1973). $J = -4 \times 10^{-5}$ (Hill & Stebbins, 1975).

PLANET	$G m (10 m^3/sec^2)$	$G m/r^3$	$G m \sin 2\theta/r^3$
Mercury	22031.8	1.3×10^{-19}	1.5×10^{-20}
Venus	324858.6	2.6×10^{-19}	$3.4 \times "$
Earth+Moon	403503.22	1.2×10^{-19}	$3.0 \times "$
Mars	42828.44	3.7×10^{-21}	0.072 "
Jupiter	126686.9×10^3	2.7×10^{-19}	5.6×10^{-20}
Saturn	37938.5×10^3	1.3×10^{-20}	0.24 "
Uranus	585×10^4	2.5×10^{-22}	0.0055 "
Neptune	686×10^4	7.5×10^{-23}	0.00016 "

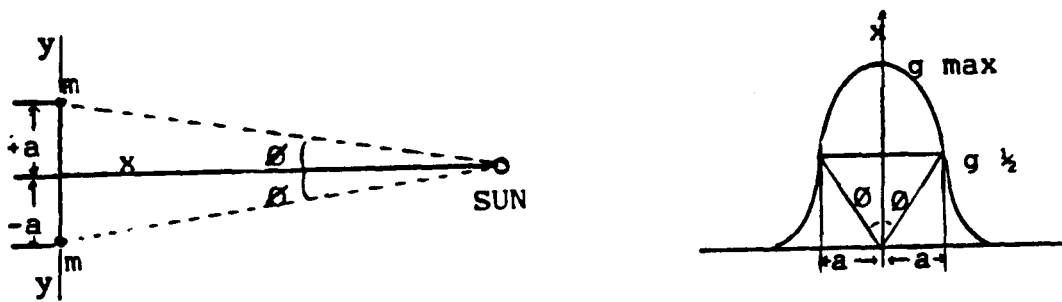


Fig. 4.3.1(a) Two point masses are situated on the y -axis at $\pm a$. Find the gravitational field along the x -axis, when $x \gg a$.
 (b) The half-value $g_{\frac{1}{2}}$ of g_{\max} . (See text).

4.3 THE COMBINED GRAVITY FIELD OF TWO PLANETS ACTING ON THE SUN

We wish to calculate the angular separation in longitude of two gravitational bodies, such that the gravitational field at a large distance perpendicular to the line joining them is one-half of the value of the two bodies superimposed (in line). This would approximate two planets in conjunction, then separated by an angle θ (both have the same mass and are at the same distance as a first approximation) (See Fig. 4.3.1).

To find the half-value of g_x , set $g_x = (1/2)g_{\max}$. Take a ratio

$$\frac{g_x}{g_{\max}} = \frac{1}{2} = \frac{-Gmx/(x^2+a^2)^{3/2}}{-Gmx/(x^2)^{3/2}} \quad (4.3.1)$$

Solve for x , calculate $\tan \theta = a/x = 0.7665$; $\theta = 37.47^\circ$.

Thus two planets of the same mass and in the same orbit separated by 37.47° longitude have one-half of the gravitational force that they would have if at the same longitude (in conjunction).

In actuality, the duration of effect of two planets in conjunction on sunspot number extends to ± 5 days, in the case of Venus and the Earth (Link et al, 1954), or about 10° , not 37° , so the Gaussian or cosine formula to be used should be a much steeper function.

4.4 NORTH-SOUTH ASYMMETRY OF SOLAR ACTIVITY

Solar activity is not equally divided between the northern and southern hemispheres of the sun. Before 1850, sunspots were more numerous in the northern hemisphere. From 1865 to 1910 they predominated in the southern hemisphere. From 1910 to 1969 there was a northern excess, with a strong asymmetry in cycle 20 (Dodson & Hedeman, 1970). Apparently in the 1980's the northern excess may have come to an end.

If sunspots (and associated solar activity) are influenced by planetary positions, then their slow swing in N/S latitude may be related to the similar slow latitude swing in the combined influence of all planets which exert an effect on the sun. Any such influence should refer to planetary latitude with respect to the solar equator. The slowest important planets, Uranus and Neptune, reached their greatest latitude north only 10 years apart in 1672 and 1682, respectively, in the solar equatorial system. The most extreme case of N/S sunspot asymmetry occurred between 1672 and 1704, when no northern spots were observed. During this entire time period two or more outer planets were north of the solar equator. Two years before Uranus reached its descending node, Saturn passed its ascending node.

The orbital period of Uranus is 84 years. The conjunction period of Saturn and Neptune is 36 years, or about half the observed long N/S period of sunspots. The Neptune orbital period is 164 years, or about twice the observed N/S sunspot period (See Figs. 4.4.1 & 4.4.2 and Table 4.4.1).

Various observers find a long period N/S oscillation of sunspot positions of 55 years (Berdishevskaya, 1967) of 70 and 84 years (Brunner-Hagger & Liepert, 1944), and 70 years (Wolbach, 1960) (White & Trotter, 1971), depending upon how it is measured.

Shown in Table 4.4.1 is the latitude of three outer planets by decades for the entire historical record of sunspot measurement. In Fig. 4.4.2 is shown a comparison of the N/S asymmetry of sunspots for the period 1943-1977 (Fracastoro & Marocchi, 1978), and the latitude of four outer planets relative to the solar equator.

Also relevant is the latitudinal position of the sun center (CS) relative to the Center of Mass of the Solar System (Petrova et al, 1978). The outer planets contribute the following percentages to the displacement of the sun: Jupiter: 49%, Saturn: 27%, Uranus: 8%, Neptune: 15%, and Pluto: 1%. The vector quantity (CS-CMSS) is related to the sun surface and sun center Coriolis acceleration (Pimm & Bjorn, 1969).

The K-corona and the zodiacal light may rotate at an inclination to the solar equator. Evidence is seen from observations of the K-corona and zodiacal light, especially when observations are made near to the axis of the nodes of the planetary system on the solar equator. The inner K-corona is inclined about 3° to the solar equatorial plane. Farther out the zodiacal cloud is inclined between 4° and 5.7° (Misconi, 1977). There would be a resulting non-uniform shear around the solar equator, which might engender oscillations. Such oscillations may have been observed, with periods of half a year (180.5 days) and half of Jupiter's synodic period (199.3 days) (Czada, 1983).

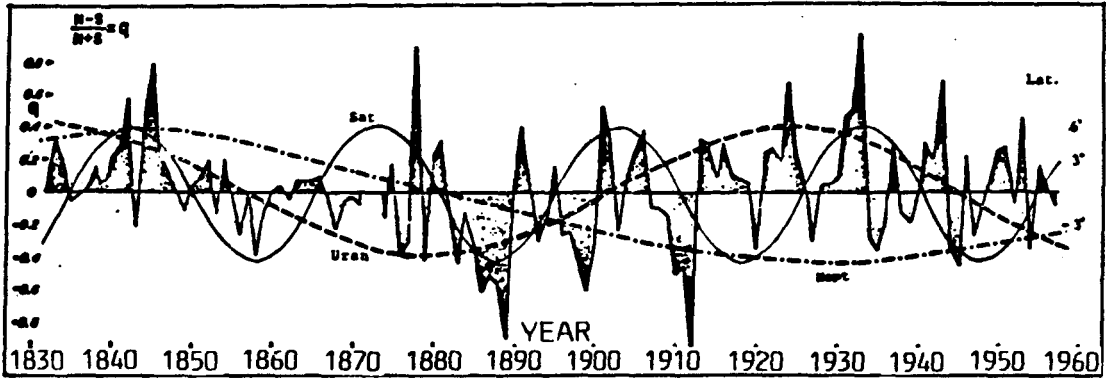


Fig.4.4.1. Relative spotted area of the north and south hemispheres, left, expressed by the ratio $q=(n-s)/(n+s)$, compared to latitude of outer planets above or below the solar equator (Wolbach, 1962).

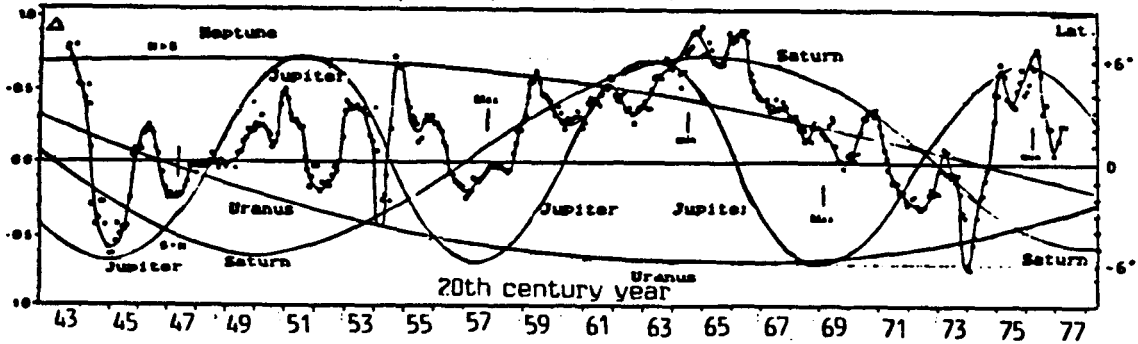


Fig.4.4.2 Monthly values of parameter Δ , the asymmetry between the activity in the north and south hemispheres 1943-1977 (left) (Fracastoro & Marocchi, 1978), compared to latitude of outer planets relative to the solar equator (right).

Table 4.4.1 Longitude of the outer planets, Jan 1 of year given, relative position north or south of the solar equator, and approximate Latitude (θ) from the solar equator.

Jan 1 Year	Saturn		Uranus		Neptune	
	N/S	λ θ	N/S	λ θ	N/S	λ θ
1790	N	353° +6°	S	128° -3°	S	204° -3°
1800	S	128° -3°	S	173° -5°	S	226° -1°
1810	S	218° -3°	S	218° -2°	N	247° 0°
1820	N	3° +6°	N	260° +1°	N	269° +1°
1830	N	135° -4°	N	303° +3°	N	291° +2°
1840	S	240° -0.5°	N	345° +6°	N	310° +4.5°
1850	N	350° +6°	N	26° +3°	N	335° +6°
1860	S	130° -4°	N	70° +0.5°	N	0° +5°
1870	S	250° -0.5°	S	111° -1.5°	N	19° +3.5°
1880	N	5° +6°	S	155° -5°	N	45° +1.5°
1890	S	140° -4.5°	S	201° -3°	S	64° -0.2°
1900	N	254° +0.5°	S	245° -0.5°	S	90° -1°
1910	N	10° +1°	N	286° +1°	S	108° -2.5°
1920	S	150° -5°	N	330° +5°	S	135° -5°
1930	N	270° +1°	N	11° +5°	S	152° -6°
1940	N	25° +1°	N	57° +1°	S	175° -5.5°
1950	S	160° -6°	S	98° -1°	S	195° -4°
1960	N	280° +1°	S	135° -4°	S	215° -2°
1970	N	40° +1°	S	185° -6°	S	238° -0.2°
1980	S	179° -5°	S	230° -1°	N	256° +0.5°
1990	N	286° +1.5°	N	271° +1°	N	283° +2°
2000	N	47° +0.2°	N	313° +4°	N	305° +4°

7 BIBLIOGRAPHY

- Allen, C. W., "Astrophysical Quantities," Athlone Press, London, 3rd ed., 1973
- Alfven, H. & Arrhenius, G., "Evolution of the Solar System," NASA SP-345, Washington, DC 1976
- "Astronomical Almanac," US GPO, Washington, DC (yearly)
- Baker, N. & Temesvary, S., "Tables of Convective Stellar Envelope Models," NASA Inst for Space Studies, NY, 2nd Ed., 1966
- Berdichevskaya, V.S., "A Periodicity in the North-South Asymmetry of the Sunspot Distribution at the Minimum of New Cycles," Sov. Astron. 11 283 (1967)
- Blizard, J.B., "Solar Activity: Long-Range Prediction," in "Climate: History, Periodicity and Predictability," Hutchinson-Ross, NY 1987
- Blizard, J.B., "Long Range Solar Flare Prediction," Final Report, NASA Contract NAS8-21436, 169 pp., 1969
- Blizard, J.B., "Precessional Effect on an Oblate Sun," B.A.A.S. 13 981 (1983)
- Brunner-Hagger, V.W. & Liepert, A., "Comparison of the Sunspot Curve for the Years 1853-1939 for the North- and South Hemispheres," Astr. Mitt. 141 556 (1941)
- Bursa, M., "Precessional-Nutational Torque of the Planets," B.A.C. 35 87 (1984)
- Campbell, L. & Moffat, J.W., "Quadrupole Moment of the Sun and the Planetary Orbits," Ap. J. 275 L77 (1983)
- Cox, J.P., "Theory of Stellar Pulsation," Princeton U Press, Princeton, NJ 1980
- Cox, J.P., & Guili, R.T., "Principles of Stellar Structure," Gordon & Breach, Inc. NY 1967
- Czada, I.K., "Evidence for the Phi-dependent Rotation-oscillation of the Sun," Sol. Phys. 82 439 (1983)
- Dodson, H.W. & Hedeman, E.R., "Time Variations of Solar Activity," p 151 in "Solar Terrestrial Physics/1970," Dyer, ed., D. Reidel, Dordrecht-Holland, 1972
- Hickey, J.R., et al, "Solar Variability Indications from Nimbus 7 Satellite Data," in NASA CP-2191, Washington, DC 1981
- Hill, H.A. & Stebbins, R., "The Intrinsic Visual Oblateness of the Sun," Ap. J. 200 471-483 (1975)
- Hoyt, D. & Eddy, J., "Solar Irradiance Modulation by Active Regions, 1969-1981," Geophys.Res.Lett.10 509-512 (1983)
- Jackson, S., "Classical Electrodynamics," Wiley NY 1976
- Jose, P.D., "Sun's Motion and Sunspots," A.J. 70 193 (1965)
- Kaula, W.M., "Introduction to Planetary Physics," Wiley NY (1968)
- Khlystov, A.I., "On the Possibility of Resonance Enhancement in the Convective Zone," Soln. Dannye #10 78 (1978)
- Link, F., "Planetary Influences on the Sun, XII," B.A.C. 6 133 (1954)
- Melchoir, P., "The Earth Tides," Pergamon Press, NY 1966

- Misconi, N.Y., "The Symmetry Plane of the Zodiacal Light near 1 AU," in "Solid Particles in the Solar System," J. Halliday & B.A. McIntosh, Ed., Reidel, Boston, 1980
- Petrova, N.C., et al, "Comparison between Time-spatial Position of the CMSS Relative to the Solar Center and Solar Activity," Soln. Dannye #12 89 (1978)
- Pimm, R.S. & Bjorn, T., "Prediction of Smoothed Sunspot Number using Dynamic Relations between the Sun and Planets," NAS8-21445 Final Report, April, 1969
- Provost, J., Berthomieu, G., & Rocca, A., "Low Frequency Oscillations of a Slowly Rotating Star: Quasi-toroidal Modes," Astr. Astrophys. 94 126 (1981)
- Saio, H., "R-mode Oscillation in Uniformly Rotating Stars," Ap. J. 256 717 (1982)
- Sanders, J.E., "Short-term Periodicity of Solar Orbital Accelerations," in Climate: History, Periodicity and Predictibility," Hutchinson-Ross, NY 1987
- Takahashi, K., "Solar-terrestrial Disturbances of August, 1972," J.Radio Res. Lab. Japan 21 459 (1974)
- Tuominen, J. et al, "Meridional Motions Derived from Positions of Sunspot Groups," MNRAS 205 691 (1984)
- Unno, W., et al, "Nonradial Oscillations of Stars," Univ. Tokyo Press, Tokyo, Japan, 1979
- Ward, F., "Circulation of the Solar Atmosphere and Maintenance of the Equatorial Acceleration," Ap. J. 141 534 (1965)
- Warwick, J., "Magnetic Fields in the Solar System," in "Magnetospheric Particles and Fields," McCormac, ed. Reidel NY 1976
- White, O.R. & Trotter, D.E., "Distribution of Sunspots Between North and South Solar Hemispheres," Ap.J.Supp. 33 391 (1971)
- Williams, G.E. & Sonett, C.P., "Solar Signature in Sedimentary Cycles from the Late Precambrian Elatina Formation, Australia," Nature 318 523-322 (1985)
- Winkler, C., et al, "Plane of Symmetry of the Zodiacal Light and Structure of the Gegenshein," Astr Astrophys. 143 194 (1985)
- Wolbach, J., "On the Unequal Spottedness of the Two Solar Hemispheres," Smiths. Contrib. 5 195 (1962)
- Wolff, C.L., "Rigid and Differential Rotation Driven by Oscillations Within the Sun," Ap.J. 194 489 (1974)
- Wolff, C.L., "Timing of Solar Cycles by Rigid Internal Rotations," Ap.J. 205 612 (1976)
- Wolff, C.L., "Rotational Spectrum of G-modes in the Sun," Ap.J. 264 667 (1983)
- Wolff, C.L., "Solar Irradiance Changes Caused by G-modes and Large Scale Convection," Sol. Phys. 93 1 (1984)
- Wolff, C.L. & Blizard, J.B., "Properties of R-modes in the Sun," Sol. Phys. 105 1 (1986)
- Wolff, C.L. & Hickey, J.R., "Multiperiodic Irradiance Changes Caused by r-modes and g-modes," Sol.Phys. 108 (1987)